Planetary Science
a SpringerOpen Journal

ORIGINAL RESEARCH Open Access

Precipitation-induced surface brightenings seen on Titan by Cassini VIMS and ISS

Jason W Barnes[1*], Bonnie J Buratti[2], Elizabeth P Turtle[13], Jacob Bow[1], Paul A Dalba[2,3], Jason Perry[5], Robert H Brown[5], Sebastien Rodriguez[10], Stéphane Le Mouélic[8], Kevin H Baines[15], Christophe Sotin[2], Ralph D Lorenz[13], Michael J Malaska[2], Thomas B McCord[4], Roger N Clark[6], Ralf Jaumann[12], Paul O Hayne[7], Philip D Nicholson[9], Jason M Soderblom[14] and Laurence A Soderblom[11]

Abstract

Observations from *Cassini* VIMS and ISS show localized but extensive surface brightenings in the wake of the 2010 September cloudburst. Four separate areas, all at similar latitude, show similar changes: Yalaing Terra, Hetpet Regio, Concordia Regio, and Adiri. Our analysis shows a general pattern to the time-sequence of surface changes: after the cloudburst the areas darken for months, then brighten for a year before reverting to their original spectrum. From the rapid reversion timescale we infer that the process driving the brightening owes to a fine-grained solidified surface layer. The specific chemical composition of such solid layer remains unknown. Evaporative cooling of wetted terrain may play a role in the generation of the layer, or it may result from a physical grain-sorting process.

Keywords: Titan, Atmosphere, Titan, Hydrology

Introduction

Dendritic networks of channels seen by *Huygens* revealed that rainfall drives surface erosion on Titan [1]. Subsequent *Cassini* observations showed that similar channels are seen globally on all types of Titan terrain [2-7]. While some channels terminate in broad alluvial fans, like those at the spot of *Huygens*' touchdown, others lead to polar seas [8,9] or dry lakebeds [10,11].

The timing of channel formation remains largely unknown. As yet there is no evidence for any of Titan's channels being presently filled with downhill-streaming liquid. Titan's atmospheric methane is being irreversibly destroyed [12,13], meaning that the channels could be vestigial – left over from a subsequently altered paleoclimatic regime. Global circulation models imply a relative paucity of rainfall at equatorial latitudes [14,15]. And the presence of sand dunes at low latitudes [16,17] is certainly consistent with Titan's equator being a desert in the present day. However soil moisture present at the equatorial *Huygens* landing site [18-20], along with the ubiquity of channels in Earth's deserts, are a reminder that rainfall-driven (pluvial) processes affect deserts despite infrequent rain events.

Heavier cloud cover, and presumably higher rainfall, occurs at the poles and at 40° latitude in the summer hemisphere [21-24]. However the correlation between clouds and surface rainfall is not obvious. Early theoretical models indicated that rain could not reach the surface of Titan owing to evaporation during its fall [25]. A more complete calculation including the effects of latent heat more recently established that rain is possible at Titan's surface [26].

Recent *Cassini* Imaging Science Subsystem (ISS) data dramatically confirmed that rain occurs on Titan through observation of regional darkenings southwest of Adiri associated with large cloud outbursts [27]. Turtle et al. (2011) [27] interpret these darkenings as pluvially derived liquid wetting of the surface. Subsequent to the rainfall event, some of the affected areas have brightened again. Interestingly, Turtle et al. (2011) [27] report that some locations within Adiri brightened to albedos higher than the values prior to their wetting.

In this paper, we use new observations from the *Cassini* Visual and Infrared Mapping Spectrometer (VIMS) and ISS instruments to further examine the brightenings

*Correspondence: jwbarnes@uidaho.edu
[1]Department of Physics, University of Idaho, Moscow, Idaho, 83844-0903 USA
Full list of author information is available at the end of the article

in Adiri and newly recognized brightening in three other tropical locations on Titan's surface. Section "Observation" describes the *Cassini* VIMS and ISS observations that we use and the state of the surface prior to the wetting event. In Section "Variation" we describe the time-evolution of the albedo of the wetted areas over the past year, with particular concentration on the brightening of the surface that occurs after the wetting-induced darkening. VIMS observations of the area allow us to evaluate the nature of the change in the spectral character of the surface, which we do in Section "Coloration". We describe possible physical processes that could be creating the brightening in Section "Discussion", and present our conclusions in Section "Conclusion".

Observation

We use both spectral mapping cubes obtained by the *Cassini* VIMS [28] and 0.938 μm images from the *Cassini* ISS [29] to identify and map surface changes, with RADAR [30] observations for geological context. We reduce the VIMS data using the standard pipeline calibration followed by geometric projection [31]. ISS images were processed following the procedures outlined by Turtle et al. (2009) [32] in the Auxiliary Material. RADAR observations use Synthetic Aperture Radar (SAR) mode σ_0 measurements obtained from the Planetary Data System (PDS). Tables 1, 2, and 3 summarize the observations that we present in this paper from VIMS, ISS, and RADAR respectively.

We focus on four different areas in which we see changes occur. From west to east, they are: Yalaing Terra, Hetpet Regio, Concordia Regio, and central Adiri (Figure 1).

Yalaing Terra

Yalaing Terra (centered at 19.5°S 324°W) is an 'island' of VIMS Equatorial Bright terrain (as described in [31]) surrounded by dunes. In general, Equatorial Bright material is topographically more rugged than dunes [33] and frequently stands higher than the dunes in altitude, causing dunes to divert around exposures [34]. We show VIMS color images of Yalaing Terra and an interpreted geologic/spectral unit map based on the VIMS data in Figure 2. In Yalaing Terra and other places that lack overlapping RADAR coverage, we only attempt spectral identification of landforms for previously identified spectral correlations – particularly 'dark blue' terrain like the *Huygens* landing site [35] and enhanced water ice in mountainous areas [3]. These spectral-only identifications are necessarily of lower confidence than those from RADAR and VIMS combined.

The changes that we will describe in Section "Variation" occurred near 36°E 18°S. This area is part of Yalaing Terra, inside the Equatorial Bright unit. Two mountain ranges, inferred from subtle blue deviations from the equatorial bright spectrum of the sort discovered empirically by Barnes et al. 2007 [3], cross the area. The eastern mountain range (labelled 'E' in Figure 2) is linear, with a north-south orientation. The western range (labelled 'W' in Figure 2) has a roughly circular shape, and thus could be the remnant of an ancient impact crater wall. The eastern range is more prominent than the western range; hence it is probably either higher, rougher, or larger in total extent.

Northeast of the eastern mountain range, between it and the dunes, lies an instance of 5-μm-bright terrain. 5-μm-bright terrain was first identified early in the

Table 1 Observations

Flyby	Date	Incidence	Sampling	Integration time
T15	2006 July 2	17°	66 km	640 ms
T17	2006 September 7	68°	18 km	72 ms
T21	2006 December 12	67°	31 km	400 ms
T31	2007 May 28	51° (C)	82 km (C)	640 ms
		7° (A)	68 km (A)	
T34	2007 July 19	44°	15 km	65 ms
T58	2009 July 8	18°	36 km	320 ms
T59	2009 July 24	18°	36 km	180 ms
T61	2009 August 25	17° (Y)	20 km (Y)	65 ms
		41° (H)	26 km (H)	
T67	2010 April 5	22° (Y)	30 km (Y)	220 ms (Y)
		37° (H)	43 km (H)	180 ms (H)
T70	2010 June 21	33° (C)	31 km (C)	120 ms (C)
		28° (A)	14 km (A)	80 ms (A)
T72	2010 September 24	30° (C)	19 km (C)	60 ms
		28° (A)	21 km (A)	
T74	2011 February 18	27° (Y)	128 km (Y)	180 ms
		41° (H)	175 km (H)	
T75	2011 April 19	33° (C)	307 km (C)	160 ms
		19° (A)	106 km (A)	
T76	2011 May 11	48° (Y)	16 km (Y)	140 ms (Y)
		34° (H)	31 km (H)	60 ms (H)
T77	2011 June 20	78° (C)	131 km (C)	160 ms (C)
		36° (A)	38 km (A)	220 ms (A)
T79	2011 December 13	18° (C)	44 km (C)	120 ms (C)
		24° (A)	13 km (A)	80 ms (A)
T80	2011 December 13	54° (Y)	52 km (Y)	280 ms (Y)
		35° (H)	58 km (H)	280 ms (H)

Here we summarize the *Cassini* VIMS observations used in this paper and their characteristics. For more information on the prime mission flybys, T0 through T44, see [39]. In some cases observations of different areas on the same flyby have different values. In those cases we indicate the regions of interest by letter designation: Y for Yalaing Terra, H for Hetpet Regio, C for Concordia Regio, and A for Adiri.

Table 2 ISS observations

Flyby	Date	Sampling	Range	Phase	Sub S/C Lat	Sub S/C Lon
T32	2007 June 14	0.9 km/pixel	148620 km	15.8°	2.3N	214.8W
–	2010 May 23	10.3 km/pixel	1720669 km	44.9°	5.2N	268.7W
T70	2010 June 22	3.8 km/pixel	635142 km	35.3°	9.0S	232.8W
–	2010 August 13	4.2 km/pixel	698726 km	17.8°	4.1S	343.3W
T72	2010 September 25	2.7 km/pixel	453767 km	36.6°	2.4S	213.2W
–	2010 September 27	7.7 km/pixel	1284920 km	44.0°	1.7S	246.9W
T73	2010 October 29	11.1 km/pixel	1847761 km	87.8°	3.6S	212.3W
–	2010 December 20	5.6 km/pixel	939466 km	56.7°	0.1N	323.2W
–	2011 January 15	6.0 km/pixel	996067 km	66.5°	0.1N	195.4W
–	2011 February 4	14.3 km/pixel	2396324 km	42.5°	0.2N	301.6W
–	2011 March 5	13.2 km/pixel	2205511 km	66.5°	0.3N	216.3W
–	2011 March 7	17.6 km/pixel	2944733 km	62.3°	0.3N	265.5W
T75	2011 April 19	2.1 km/pixel	347807 km	15.9°	0.2N	211.7W
T75	2011 April 20	3.7 km/pixel	612711 km	16.5°	0.2N	222.9W
T75	2011 April 25	20.1 km/pixel	3350112 km	47.5°	0.3N	308.5W
T77	2011 June 11	16.7 km/pixel	2785985 km	58.4°	0.3N	274.2W
T77	2011 June 21	2.8 km/pixel	464217 km	21.4°	0.0N	219.5W
T77	2011 June 22	4.9 km/pixel	826492 km	19.3°	0.0N	232.8W
T77	2011 June 24	13.3 km/pixel	2220314 km	10.1°	0.1N	274.6W
T77	2011 June 26	18.8 km/pixel	3141761 km	16.8°	0.2N	303.3W
–	2011 July 11	10.7 km/pixel	1786348 km	53.0°	0.2S	338.3W
–	2011 August 9	8.4 km/pixel	1407416 km	34.7°	0.3N	179.1W
–	2011 August 13	16.8 km/pixel	2808457 km	22.6°	0.2N	282.3W
–	2011 August 29	18.6 km/pixel	3113971 km	13.9°	0.2N	309.0W

Here we summarize the *Cassini* Imaging Science Subsystem (ISS) observations used in this paper and their characteristics.

Cassini mission [36-38], and its spectrum is consistent with either very low or zero water-ice content. Its specific nature as dry lakebeds of evaporite, however, was only recently proposed [11]. We interpret that this area, too, represents an evaporitic dry-lake deposit.

Hetpet Regio

Hetpet Regio (centered at 22°S 292°W) is a 'peninsula' of Equatorial Bright terrain that extends into the dunes from the south. VIMS coverage of this area during the prime mission [39] included a single observation at very coarse spatial resolution on T34 (the 34th close *Cassini* flyby of Titan, which occurred on 2007 July 19). The best views of this area prior to the changes were on T61 (2009 August 25) and T67 (2010 April 5). We show the T61 view along with an interpretation of the area's geology in Figure 3.

Even in the *Cassini* Equinox mission (2008 July through 2010 October), VIMS views of Hetpet Regio are of relatively coarse spatial resolution and have high emission angles (see Table 1). The map in Figure 3 is a best guess based on this limited information. *Cassini* RADAR from T21 covers the western portion of this study area.

The area is mostly free of high mountains. The dunes end at the northern edge of the change area, and cross it in one case. This area is bordered on the west, and possibly on the east as well, by the rarest of Titan surface spectral units: bright blue terrain (as from [31]). The bright blue spectral unit shows a higher signature of water ice than other areas on Titan [31], a characteristic that it shares with the dark blue unit (outwash plains, like at the *Huygens* Landing Site [35]). Presumably the bright blue

Table 3 RADAR observation

Flyby	Date	Area covered
T8	2005 October 28	Adiri
T21	2006 December 12	Hetpet Regio
T61	2009 August 25	Adiri

This table identifies the *Cassini* RADAR SAR swaths that we use to provide geological context for the surface change areas.

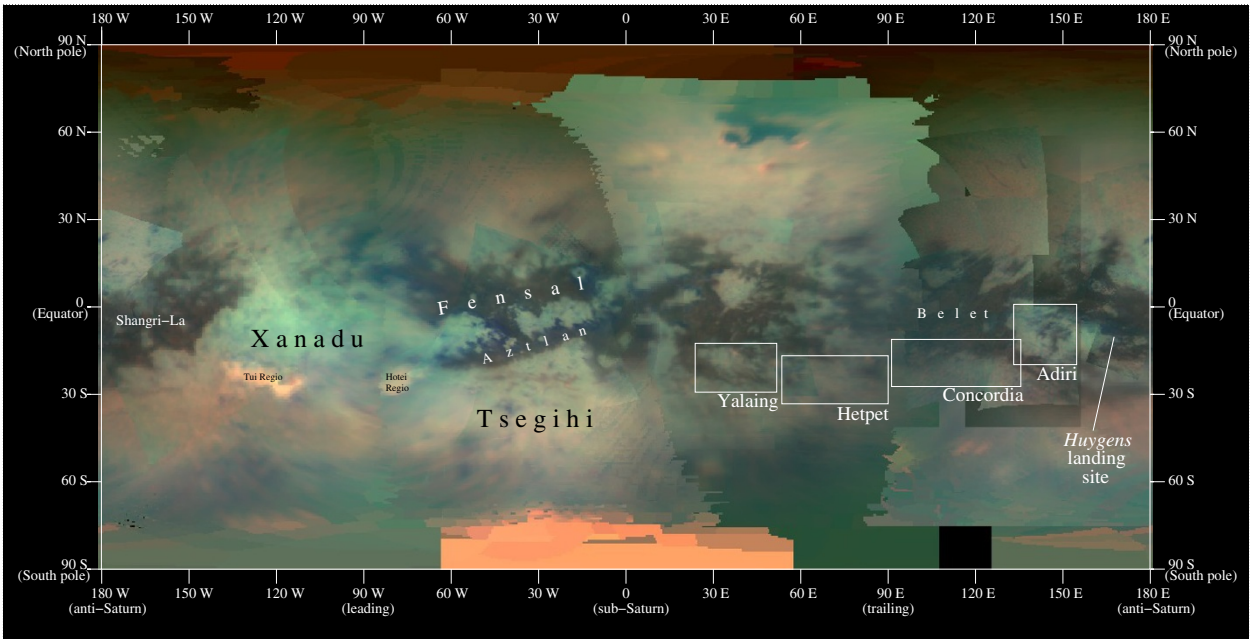

Figure 1 Geographical overview. Cylindrical overview map of Titan from VIMS, with the areas of change detection shown in Figures 6, 10, 13, and 18 denoted.

differs from the dark blue in that it has a thinner or less extensive coating of dark organic material on it, but little else is known about bright blue terrain. The central portion of the Hetpet Regio change site consists of Equatorial Bright material.

Concordia Regio

Concordia Regio (centered at 20°S 241°W) is the area in which Turtle et al. 2011 [27] observed large-scale surface darkening in late September or early October of 2010, correlated with cloudburst events. We show a VIMS mosaic from this area on T72 (2010 September 24), along with a geologic interpretation, in Figure 4.

In the north of this image is the Belet sand sea. Concordia Regio extends into the dunes from the south as an instance of Equatorial Bright [31] terrain. Several areas show slight enhancements in water ice. VIMS' spatial resolution and signal-to-noise here are insufficient to break the degeneracy between those icy areas being mountains or channels. Future observations could shed more light on the geology of this area. Concordia Regio is of particular interest given the changes seen by Turtle et al. 2011 [27] and those that we describe herein.

Central Adiri

The final area of interest is located near the center of the bright albedo feature Adiri (centered at 10°S 210°W), a thousand kilometers west of the *Huygens* Landing Site. Of our four study areas, Central Adiri is the only one where RADAR coverage overlaps locations where the surface changed. Synthetic Aperture Radar (SAR) swaths crossed this area during T8 [40] and on the T61 (2009 August 25) flyby as well. We show the RADAR data, along with VIMS coverage from T31 and T70, in Figure 5.

The bright albedo feature Adiri itself represents an instance of the VIMS Equatorial Bright spectral unit typical of those parts of Titan's tropics that are not covered in dunes. Adiri is surrounded by sand seas, with Belet to the west and Shangri-La to the east. Unusually for large Equatorial Bright regions, Adiri also has sand dunes within its extent. The four central dunefields have been assigned the names Eurus Undae, Boreas Undae, Kajsa Undae, and Notus Undae after the Greek gods of the eastern, northern, western, and southern winds respectively (Figure 5, lower-left panel).

We identify mountains in the SAR data using the techniques outlined in [41] – primarily via bright-dark line pairings indicative of layover of topography in delay-Doppler space. Adiri is highly mountainous [41]. The mountains here are primarily linear or curvilinear. Their orientations are broadly east-west. The mountains interact with the interspersed dunefields in a complex pattern, sometimes delineating the margins of dunefields and sometimes intruding into them. The identification of mountains in the unit map in Figure 5 is the most certain of any of the areas due to the presence of RADAR data and VIMS coverage with both high signal-to-noise and moderate spatial sampling (14 km/pixel). For ease of reference,

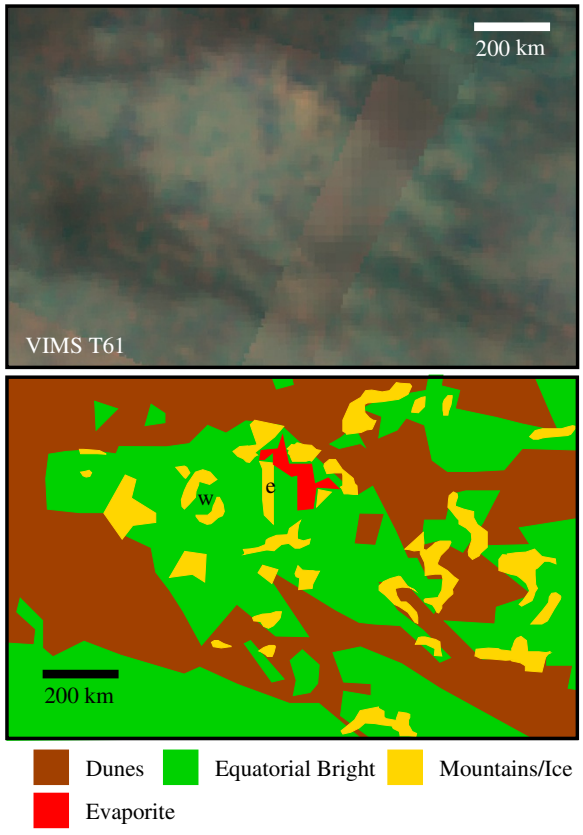

Figure 2 Yalaing Terra geology. This figure shows a geological interpretation of Yalaing Terra before the change event, using an orthographic projection from above. Brown indicates dunes, green is equatorial bright material, yellow mountainous regions, and red indicates evaporite.

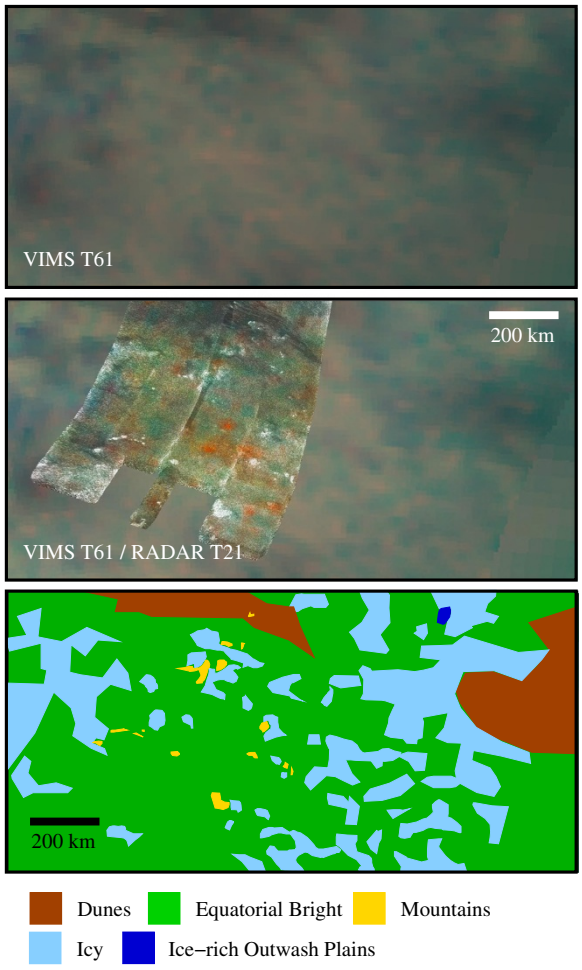

Figure 3 Hetpet Regio geology. This figure shows a geological interpretation of Hetpet Regio before the change event, using an orthographic projection from above. Brown indicates dunes, green is equatorial bright material, yellow mountainous regions, light blue regions of locally enhanced water-ice content, and blue water-ice-rich outwash plains like the *Huygens* landing site.

six of Adiri's mountain ranges in our study area have been named as we indicate in Figure 5 (lower-left panel).

Variation

All of our study areas show roughly the same pattern of brightness changes, centered on the 2010 September cloudburst, but occurring with slightly different timescales. Here we examine the time-evolution of each area in individual detail, before inferring general trends.

Yalaing Terra

We show three-color VIMS surface images of Yalaing Terra (centered near 34°E 17°S) over the course of the *Cassini* mission in Figure 6. Figure 6 shows that the area was static from the first VIMS view on T15 (2006 July 2) through high-quality observations on T61 (2009 August 25) and T67 (2010 April 5).

On T76 (2011 May 8), VIMS sees several large regions that have brightened beyond their original Equatorial Bright albedo spectrum. The areas are tens to hundreds of kilometers across, with at least seven distinct, separated areas having brightened. VIMS' only intervening view between T67 and T76 was on T74 (2011 February 18). The T74 observations were of rather coarse spatial resolution, and hence are inconclusive, but appear to show that the brightening had already occurred by the time of that flyby.

ISS observes Titan more frequently than just on the close flybys. The finer angular resolution of the ISS Narrow Angle Camera (NAC) allows moderate-spatial-resolution, full-disk Titan imaging from distances over 3 million kilometers. During both the Equinox and Solstice extended missions, *Cassini* ISS observes Titan every few weeks in the Titan Meteorological Campaign (TMC) in order to monitor cloud activity. In so doing, ISS resolves the recent surface changes in Yalaing Terra in time,

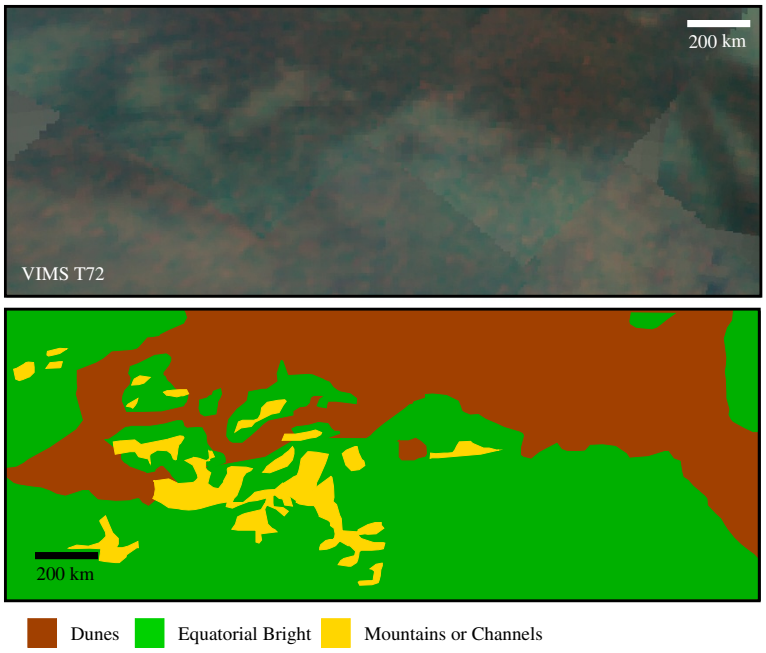

Figure 4 Concordia Regio geology. This figure shows a geological interpretation of Concordia Regio before the change event, using an orthographic projection from above. Brown indicates dunes, green is equatorial bright material, yellow areas with minor enhancement in water ice that could be either channels or mountainous regions.

complementing the ability of VIMS to resolve them in wavelength (spectrum). Because TMC observations occur between numbered close Titan flybys, they do not have a T-number associated with them.

No ISS observations of Yalaing Terra were acquired during the critical time period when Turtle et al. [27] originally saw a cloudburst and surface darkening in Concordia Regio in 2010 October, due to unfavorable spacecraft/Titan geometry. However, we show a time sequence of the time evolution of Yalaing Terra in relative brightness from 2010 December 20 through 2011 August 29 in Figure 7. We show schematic maps of the changed areas inferred from those images and those from VIMS in Figure 8.

The first image in the sequence, from 2010 December 20, shows both brightening and darkening in Yalaing Terra, both changes from the original, pre-cloudburst albedo spectrum. Darkening occurs both in the eastern end of Yalaing Terra and in the north-central area that we interpret as evaporite in Figure 2, consistent with ephemeral ponding in a local basin. A larger area centered 300 km west of the evaporite shows more modest but still significant surface darkening as well, perhaps from surface wetting as seen elsewhere [27].

Brightened areas exist directly contiguous with darkened areas. ISS sees that the surface has brightened immediately surrounding the larger moderately darkened area to the west, south, east, and northeast. These brightenings appear only in VIMS spectral units identified as Equatorial Bright terrain. The brightenings avoid the areas richer in water ice that could be mountains or icy plains.

By 2011 April 25, the large, moderately darkened area has disappeared. Instead, much of that area is now brightened instead, beyond its original albedo. Most of those previously brightened areas are still brightened, but some on the periphery have reverted to their original ('Equatorial Bright') state.

Later observations show brightened areas with similar extent to those identified by VIMS on T76 (2011 May 8). The brightest areas seen by VIMS on T76 occur in the same area that ISS identified as moderately darkened on 2010 December 20. The brightened areas appear to be drawing inward to smaller and smaller spatial extents over the course of many months, with the areas first identified as moderately dark and those that were brightest persisting for longest. The instance of the evaporitic spectral unit seen by VIMS prior to the cloudburst of 2010 September is no longer evident on T76.

Our most recent observation from VIMS, on T80 (2012 January 2), though of modest resolution, shows the least areal extent of brightening since T67. Despite the modest quality of the observation, the evaporite deposit is again visible on T80, implying that whatever process prevented it from being visible on T76 no longer does so.

We quantify the apparent brightness curve for the brightened area from ISS in Yalaing Terra in Figure 9.

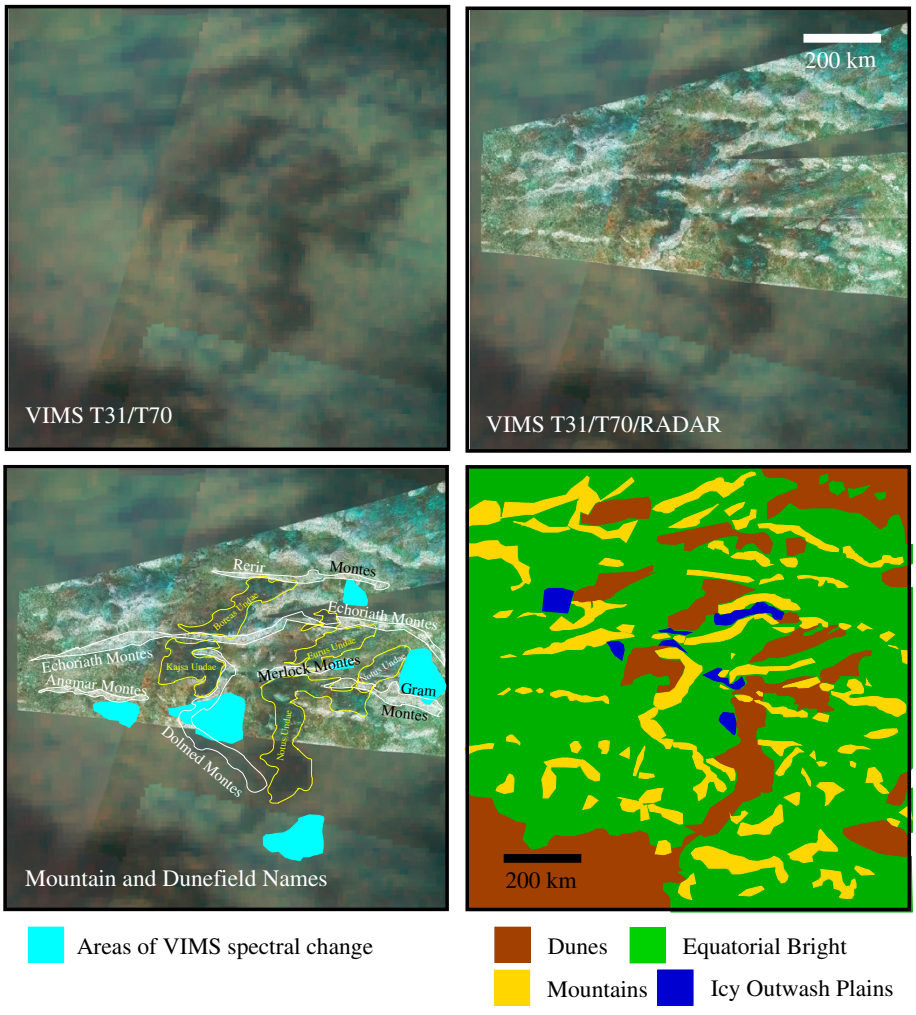

Figure 5 Central Adiri geology. This figure shows a geological interpretation of the Central Adiri area before the change event, using an orthographic projection from above Adiri. Brown indicates dunes, green is equatorial bright material, yellow mountains, and blue icy outwash plains. Identification of mountains within the area with RADAR coverage is necessarily of higher fidelity than the identification of mountains from VIMS alone. At bottom left we also indicate the areas where VIMS sees surface changes in order to place them into context with the map.

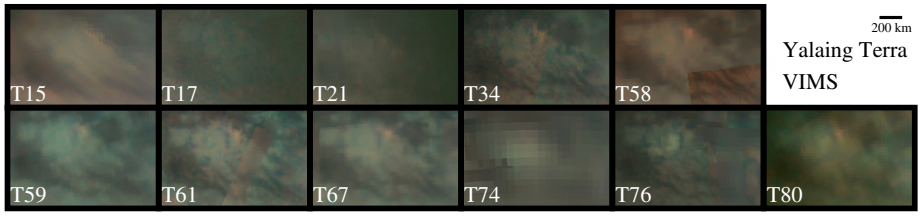

Figure 6 Yalaing Terra changes. Here we show multiple views of Yalaing Terra as seen by *Cassini* VIMS over the course of the mission to date. Each is displayed in orthographic projection from above Yalaing Terra and colored such that the red channel corresponds to the VIMS view at 5 μm, green at 2 μm, and blue at 1.3 μm (as in [31]). Accounting for changes in viewing and illumination geometry, the area was static in albedo and spectrum from *Cassini*'s arrival through flyby T67 (2010 April 5). VIMS' next quality view of the area, on T76 (2011 May 8) shows evident changes. An intervening observation on T74 (2011 February 18) seems to show brightening, but its spatial resolution is sufficiently coarse as to make the detection nondefinitive. By T80 (2012 January 2), the brightening has reduced in spatial extent. The evaporitic deposit (orange here) disappeared on T76, but is visible again on T80 (on T74 the spatial sampling is insufficient to either identify or rule out the presence of the evaporite deposit).

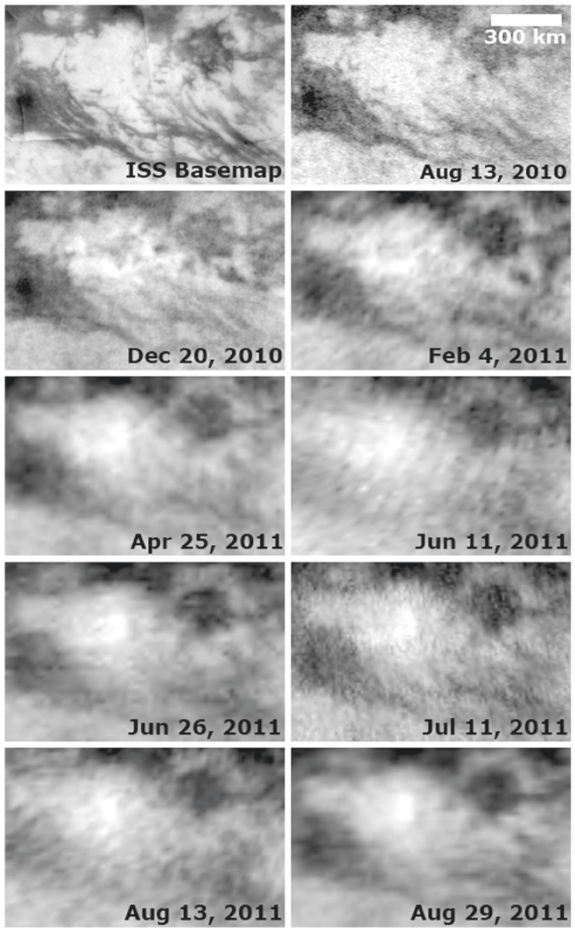

Figure 7 Yalaing Terra time evolution. This figure shows the time evolution of Yalaing Terra as seen by *Cassini* ISS from 2010 August (before the changes occurred) through 2011 August 29. The ISS Basemap is a mosaic of the best ISS 0.938-micron images of each individual area over different flybys stitched together. High-cadence temporal resolution from ISS nicely complements the spectral resolution that VIMS affords. The earliest post-event observations show both highly darkened, moderately darkened, and brightened areas. The darkest areas revert to their original brightness over several months. The brightened areas revert more slowly, and moderately darkened areas turn bright and then slowly fade.

Because the images obtained by ISS contain a complex convolution of atmospheric and surface contributions, absolute albedo calibration is not possible. Observation geometry strongly affects ISS photometry (see Table 2 for the geometry of each ISS observation). We compensate for geometry empirically, following [42], but residual systematic errors resulting from incomplete processing likely remain. In order to minimize these errors, we took two static areas, one dark and one bright, and calibrated each image individually assuming a linear relationship with the dark area assigned a 'relative reflectivity' R_{dark}=0.0, and the bright area $R_{\mathrm{bright}} = 1.0$. We then assume that surface reflectivity behaves linearly as a function of ISS-measured I/F, and assigned values for the brightness of Yalaing Terra accordingly, with

$$R = \frac{V - V_{\mathrm{dark}}}{V_{\mathrm{bright}} - V_{\mathrm{dark}}} \quad (1)$$

where V represents the measured brightness value of each respective area in the processed ISS image, and R represents the relative reflectivity as defined. The resulting curve matches the qualitative description of albedo changes as described previously.

Hetpet Regio

Our second study area, Hetpet Regio (centered near 72°E 22°S), is 1600 km east of Yalaing Terra. Like Yalaing Terra, historical VIMS observations acquired over the full *Cassini* mission confirm that the area was static until sometime between T67 (2010 April 5) and T74 (2011 February 18). We show before and after views in Figure 10 for comparison. In Hetpet Regio, a swath of Titan's surface also brightened as seen by VIMS. This change was approximately 3.5 times more extensive in surface area than the Yalaing Terra changes.

As was the case for Yalaing Terra, the brightening in Hetpet Regio occurred across the near-infrared spectrum, in each of Titan's atmospheric windows where VIMS can see down to the surface. In Figure 11 we show two spectral ratios in order to illustrate the wavelength independence of the changes. One ratio compares the Hetpet Regio change region outlined in Figure 8 to a nearby, unchanged area both on T76. The other ratio compares the area that shows changes on T76 to its pre-change state during T61. Both ratios broadly agree, and show that significant, real surface brightening had occurred on Titan at 0.938, 1.08, 1.28, 1.6, 2.0, 2.7, 2.8, and 5 micron wavelengths.

Cassini/ISS also has TMC observations of Hetpet Regio, as shown in Figure 12. The ISS data show evidence for an event between 2010 May 23 and 2010 December 20. Though the 2010 December 20 data have incomplete coverage and low signal-to-noise, they, along with the much better 2011 February 4 observations, show both brightened and darkened areas.

Over the ensuing months many of the darkened areas become brightened areas – not just reverting, but brightening beyond their original reflectivity significantly. By T80 (2012 January 2), the total contrast that the Hetpet Regio brightening shows relative to its surroundings decreased as seen by VIMS. The coarse spatial resolution coverage makes analysis of the extent of the brightenings ambiguous from VIMS T80.

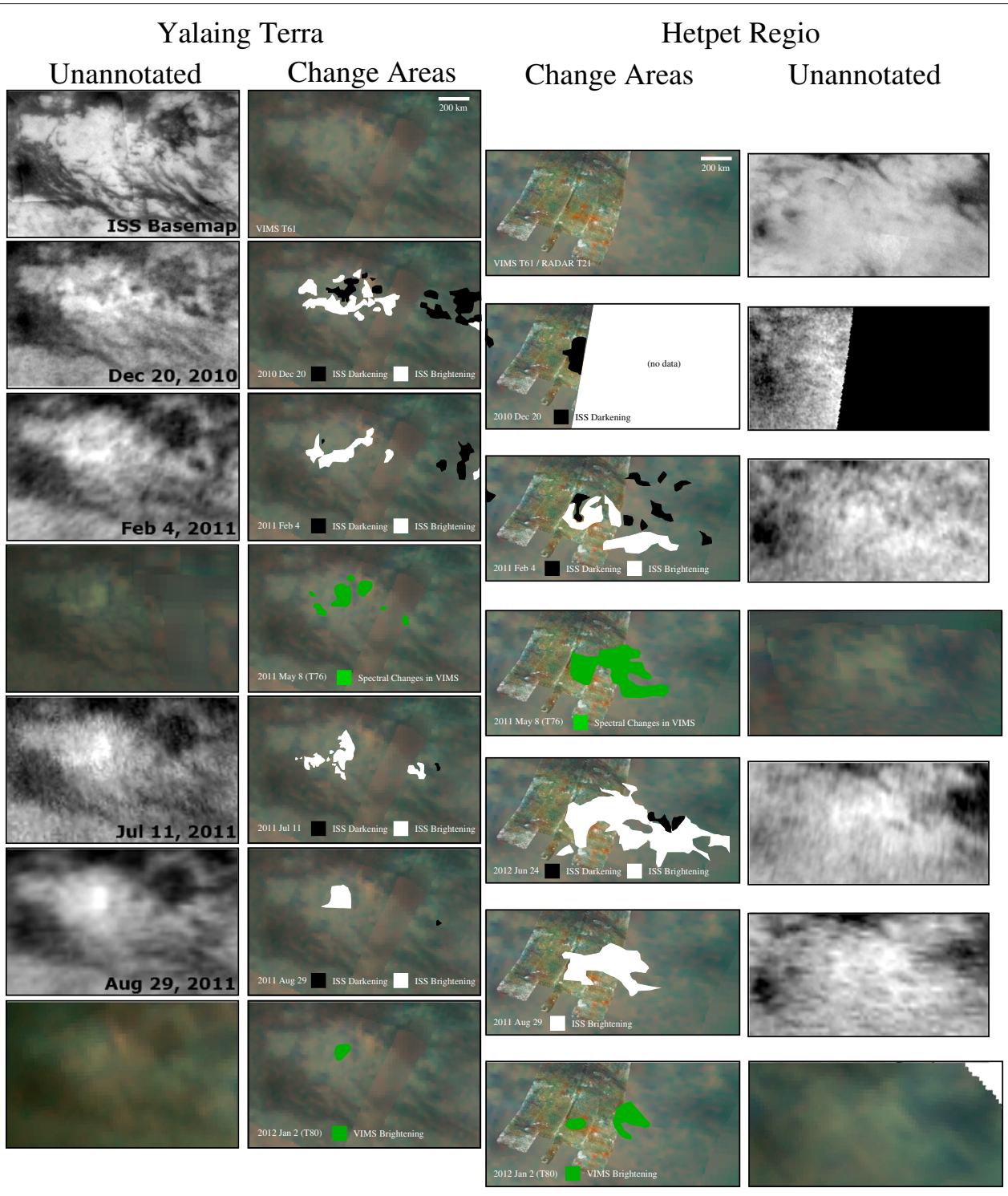

Figure 8 Yalaing Terra and Hetpet Regio change sequence. Here we document the changed areas in Yalaing Terra and Hetpet Regio that occurred over the course of late 2010 through 2011 August as seen by both VIMS and ISS, with VIMS T61 combined with RADAR from T21 where available for comparison and context. Changes are identified relative to the pre-cloud-outburst state. We have taken care to identify potentially changed areas conservatively – hence the actual changes may extend beyond those areas that we identify here.

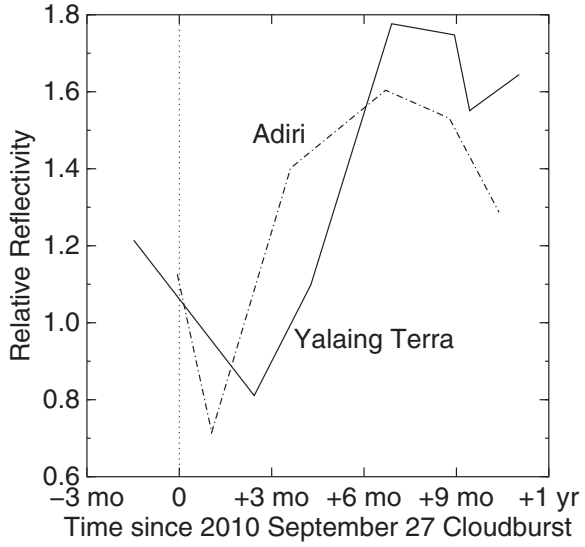

Figure 9 Yalaing Terra and Adiri lightcurves. We plot here the relative reflectivity of the brightened areas in both Yalaing Terra (solid line) and Adiri (dot-dashed line) as a function of time relative to the 2010 September 27 cloudburst recorded by [27]. We arrived at each data point by calculating the average image value in a dark area ($V_{\rm dark}$), a light unchanged area (V_{bright}), and the brightened area (V), and assigning the relative reflectivity R to be $\frac{V-V_{\rm dark}}{V_{\rm bright}-V_{\rm dark}}$. These two regions show the same pattern of initial darkening for a few months and then brightening beyond their original reflectivity for about a year. We have plotted the brightness trajectory of the cores of the change areas here. While these cores have not yet reverted to their original brightness, the periphery of the change areas have completely reverted as of 1 year beyond the cloudburst.

Concordia Regio

Concordia Regio is the location where Turtle et al. (2011) saw extensive tropical surface darkening in mid-late 2010 [27]. VIMS has limited high-quality observations of the area; we show the best views from both before and after the 2010 September 27 cloudburst event [27] in Figure 13. Although darkened areas are not easily identifiable in the VIMS views, VIMS does see brightening in the southern portion of the rain-darkened zone seen by ISS on 2010 October 29. The brightened area visible to VIMS is $\sim$ 1000 km long, extending roughly east-west.

ISS has much higher-quality views of Concordia Regio (Figure 14). Temporally bracketing views from 2010 September 27 and 2010 October 14 constrain the initial alteration event to have occurred during that timeframe [27]. The extensive darkened areas shown in the 2010 October 29 ISS view (Figure 14) were attributed to methane-wetting of the surface by rainfall [27].

Turtle et al. (2011) [27] first saw brightening in the southeast portion of the area that was rain-wetted on 2010 October 29 (see [27] supplemental online material). Multiple observations separated by 15 hours showed that the brightening was surficial, and not atmospheric in nature. Given the other cotemporal brightenings in Yalaing Terra, Hetpet Regio, and Adiri (see next subsection, "Adiri") over the ensuing months, the initial brightening in the wake of the 2010 October 29 darkening is evidently part of a larger geographic event.

The ISS view on 2011 April 20 gives us perhaps our best view of the fine spatial structure of the surface changes. At the west end are remnant darkened areas. The brightenings just east of those are most significant at the north and south ends, with a less brightened patch running east-west through the middle. Near the eastern end, small very dark patches a few tens of km in size are surrounded by brightened zones. Those very dark patches may represent areas where rainfall has ponded and not yet evaporated or infiltrated since 2010 October. We diagram the surface changes seen by ISS and VIMS in Figure 15, and present a cartoon of the observed change sequence in Figure 16 to illustrate the changes graphically.

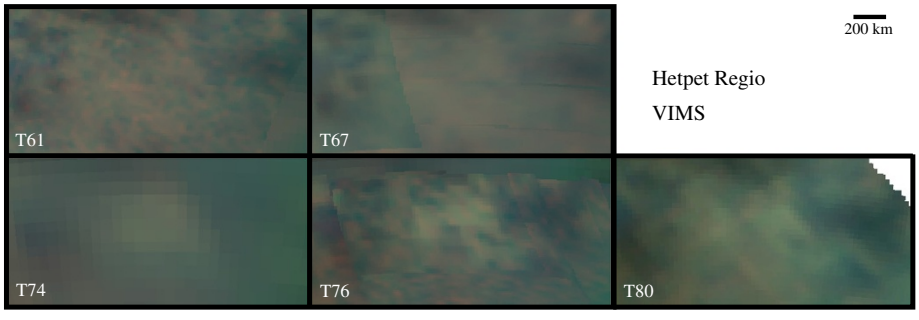

Figure 10 Hetpet Regio changes. This figure shows VIMS views of Hetpet Regio before (T61, T67) and after (T74, T76) the 2010 September 27 cloudburst event. VIMS' best view of the area post-event was on T76 (2011 May 8), with very coarse resolution but compelling evidence for the brightening also having been present on T74 (2011 February 18). Both the viewing geometry and spatial resolution for both of these observations of Hetpet Regio are of lower quality than the conditions for Yalaing Terra on those same flybys, as detailed in Table 1. Hetpet Regio is still brighter than its surroundings on T80 (2012 January 2), but shows less contrast than it did on T76.

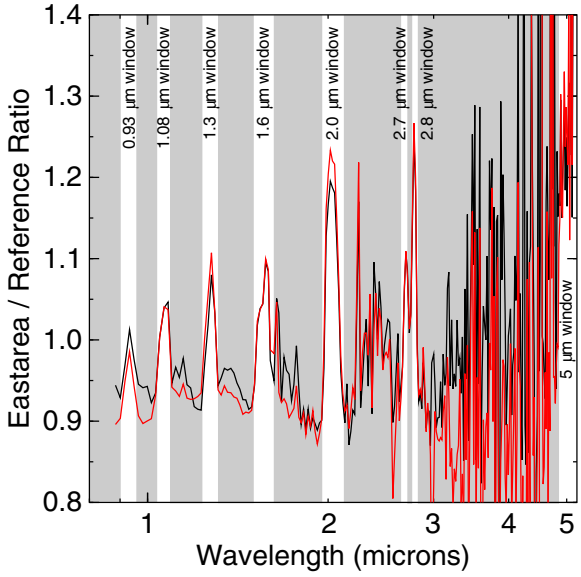

Figure 11 Spectral ratio. Here we show two spectral ratios of Hetpet Regio: in black, one between the area VIMS sees as changed and a nearby, unchanged area, both on T76; and in red, a ratio between the changed area from T76 and the same area back on T61. The areas between the spectral limits of Titan's infrared spectral atmospheric windows are indicated in white. The ratio between the spectral windows (in grey) is meaningless because the surface cannot be detected from orbit at those wavelengths. This ratio shows that the brightening occurred at all wavelengths where the surface is visible to VIMS (though the displayed ratio is contaminated by atmospheric scattering at the shortest-wavelength windows).

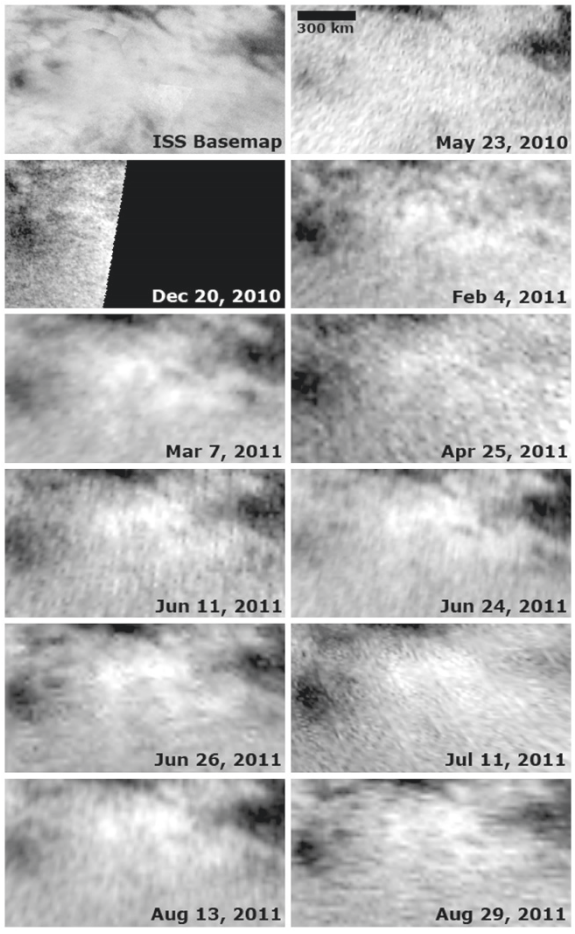

Figure 12 Hetpet Regio time evolution. ISS time-sequence for the evolution of surface brightness in Hetpet Regio from mid-2010 through 2011. Similar to Yalaing Terra, a dark-then-light paradigm holds through much of the change region. The brightest areas that show the greatest persistence of change are greater in areal extent than those from Yalaing Terra.

Adiri

Our best opportunity to place the changes that we see into local context are within Adiri. There, high-quality imaging from VIMS (T70, T77, T79), ISS, and RADAR (T8 and T61) all coincide, giving us the best opportunity to constrain the processes driving surface change.

ISS imaging (Figure 17) just a month after the 2010 September 27 cloudburst shows surface darkening in four separate areas: (1) a large, irregularly shaped area located east of Dolmed Montes and west of Notus Undae, (2) a small spot ∼20 km across located at the western edge of Kajsa Undae, and (3&4) two large areas at the southern edge of Adiri adjacent to the neighboring Belet sand sea. Data from 2010 October 29 cover just the western portion of this study area, so more darkened areas may have existed but escaped detection.

By 2011 January 15 most of the altered areas had brightened, but with one moderate-sized darkened area still southeast of Notus Undae. That darkened area is flanked to both the ENE and WSW by similarly sized brightened areas. The previously darkened zones in south Adiri adjacent to Belet became brightened areas. The previously darkened region between Dolmed Montes and Notus Undae had by then also become brightened relative to its original, pre-cloudburst state. A larger brightened area west of Dolmed Montes extends for 250 km to the south of the Angmar Montes range and parallel to it. Along the eastern part of this study area there is a large brightened region located between Echoriath Montes and Gram Montes, east of the eastern lobe of Notus Undae. And some smaller brightened surfaces exist either in or adjacent to the eastern end of Merlock Montes.

The 2011 January 15 configuration changed little in the ensuing two observations, from ISS on 2011 April 19 and from VIMS on 2011 June 20 (Figure 18). A later VIMS view on T79 (2011 December 13) shows a dramatic decrease in the area of brightened terrain. Due to the spectral character of the brightening, it can be more evident in alternate color schemes using the VIMS spectral mapping

Figure 13 Concordia Regio changes. VIMS views of Concordia Regio from prior to (T31, T64, T70) and subsequent to (T75, T77) the 2010 September 27 ISS-documented cloudburst [27]. VIMS views of this area are of generally low quality due to *Cassini* flyby geometries as constrained by the orbital mechanics of the tour. Brightening is evident in the coarse-spatial-resolution observation on T75, and is better resolved on T77. The bottom-right panel is a view from T79.

data, as we depict in Figure 19, which uses 2.0 μm for red, 2.7 μm for green, and 2.8 μm for blue.

The ISS observations for this area are of sufficient quality to measure relative reflectivity as a function of time, shown in Figure 9. The overall evolution in surface reflectivity for Adiri tracks well with that in Yalaing Terra. Adiri seems to evolve faster, though, brightening before Yalaing Terra and beginning to revert to normal at +9 months.

Coloration

In addition to brightness and morphological information, the VIMS observations of our four change areas contain spectral information. Here we use that spectral information to constrain the altitude and composition of the changed regions.

The frequent ISS observations of the four areas (Section "Variation") show consistency in the geographic locations of the changes, along with slow changes in the brightness of each area following the same pattern. The geographic stability of the areas over time implies that the changes are surficial and not atmospheric.

VIMS spectra of the changed regions agree that they are inconsistent with clouds. At the top of Figure 20, we show spectra of the changed and unchanged parts of Hetpet Regio and compare them to the spectrum of a cloud from the T33 flyby (2007 June 29). As is evident from the figure, the brightening in Hetpet Regio occurred exclusively within the atmospheric windows to the surface. In particular, at the spectral wings of the atmospheric windows, where clouds in the upper troposphere show distinctive and significant brightening over surface features (arrows in Figure 20), the changed region is static, as would be expected if it were purely a surface phenomenon. Griffith [43] and others have used similar altitude discriminators, particularly at the longward end of the 2-micron window.

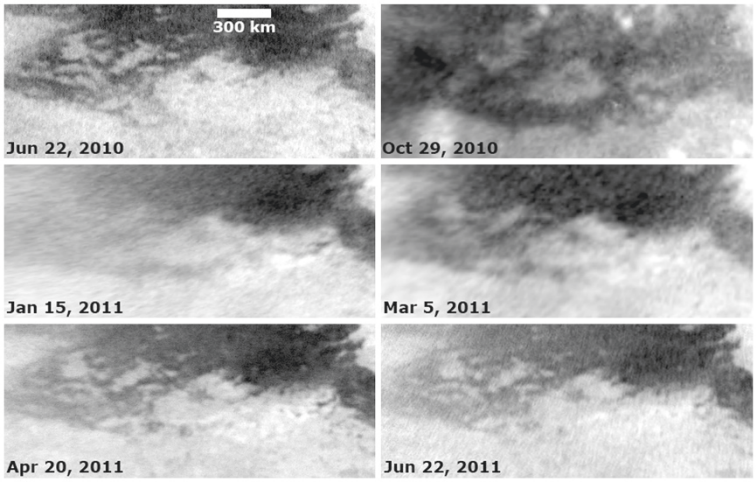

Figure 14 Concordia Regio time evolution. ISS has generally fine spatial-resolution coverage of Concordia Regio that first revealed the extensive surface darkening in the wake of the 2010 September 27 cloudburst event [27]. The 2010 October 29 observation in particular was investigated in detail by Turtle et al. 2011 [27]. Although temporal-resolution coverage of the area is coarser than for Yalaing Terra and Hetpet Regio, the high signal-to-noise and fine spatial resolution of these views reveal what may be areas of surface ponding only tens of km across surrounded by brightened terrain (2011 April 20).

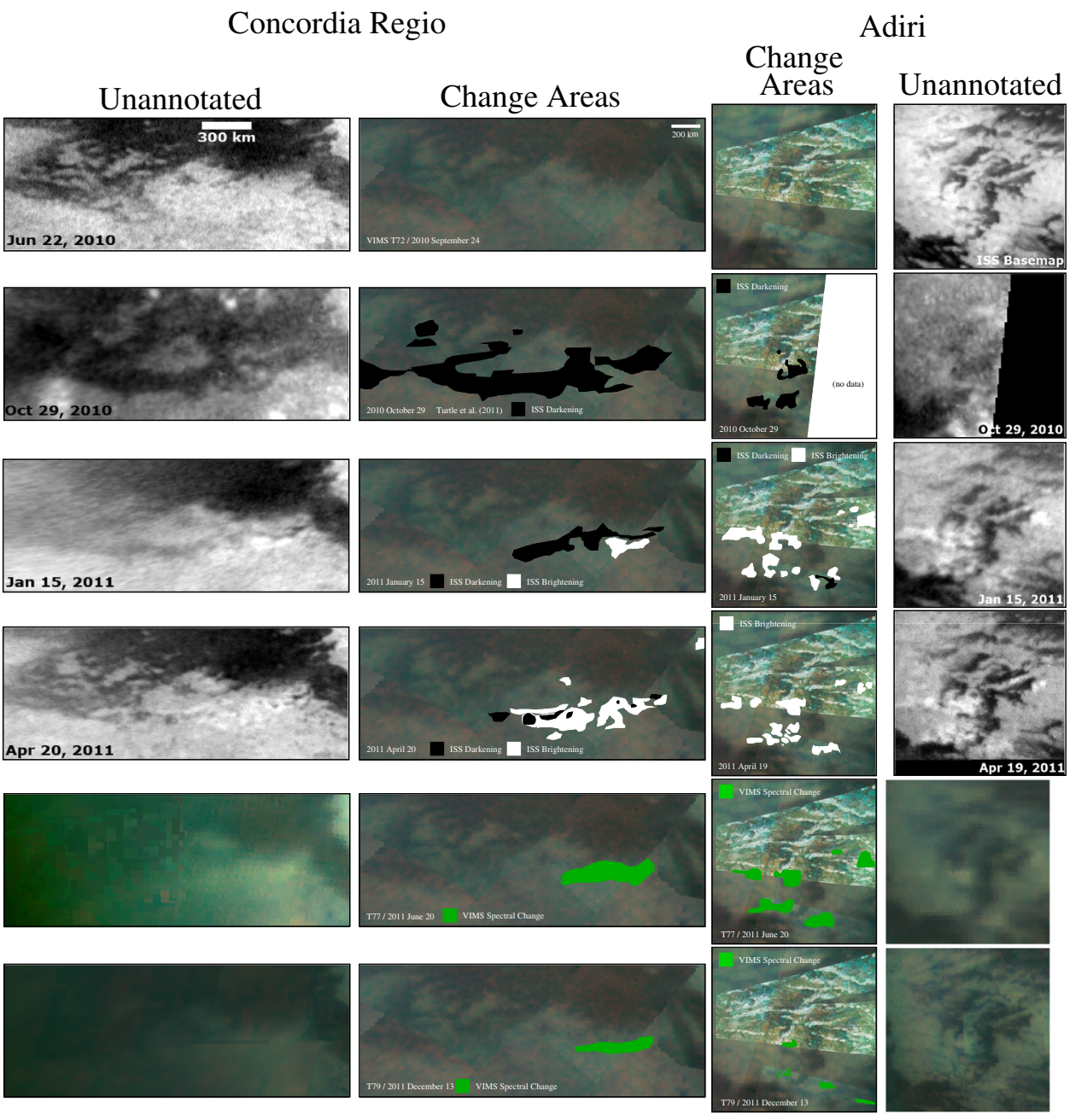

Figure 15 Concordia Regio and Adiri change sequence. Here we document the changed areas in Concordia Regio (left column) and Adiri (right column) that occurred over the course of late 2010 through 2011 August as seen by both VIMS and ISS, with VIMS T31, T70, and T72 combined with RADAR from T21 where available for comparison and context. Changes are identified relative to the pre-cloud-outburst state. We have taken care to identify potentially changed areas conservatively – hence the actual changes may extend beyond those areas that we identify here.

The relative I/F of each of the brightened areas within the spectral windows is also inconsistent with clouds. Figure 21 shows the integrated I/F for the Yalaing Terra brightened pixels from T76 compared against Equatorial Bright terrain, dark brown terrain (dunes), and clouds, all with the same viewing geometry. The T76 brightenings plot outside the bounds of normal Equatorial Bright terrain, but also fall well outside the region associated with clouds. Because this in-window test depends more highly on the target's spectrum and less on its altitude, it allows us to rule out near-surface ground fogs as well as high clouds. The longevity and temporal consistency of the changed features is likewise inconsistent with fog.

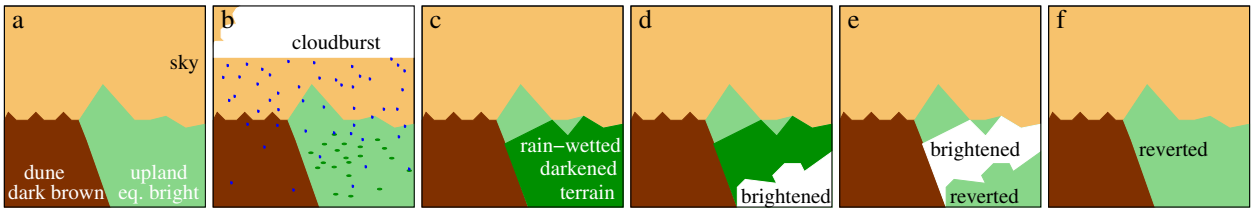

Figure 16 Cartoon of change sequence. In this figure we illustrate the observed sequence of albedo changes in cartoon form. Subfigure **(a)** shows the surface prior to the 2010 September cloudburst, and subfigure **(b)** shows it during the cloudburst. The rainfall associated with the cloudburst wets areas of Equatorial Bright terrain (and some dune areas as well), darkening them **(c)**. As the liquid dissipates, brightened areas with higher reflectivity than displayed originally appear in areas that had been previously darkened **(d)**. In **(e)**, some areas of brightened terrain have reverted to their pre-cloudburst state, while others that had stayed darkened for longer are now experiencing brightening. Finally in **(f)**, the entire area has reverted to its pre-cloudburst state.

Viewing geometry significantly affects Titan spectra. To maximize the interpretability of intercomparison we therefore use observations with as nearly identical observing geometry as possible. In particular, we elect to use the cloud on T33 as a comparison, based on the incidence and emission angles from the T76 Hetpet Regio geometry (i=31°, e=47°), having searched the entire VIMS dataset for points on each flyby that had identical geometry. In general, there is at least one such point for each flyby (though their phase angles will differ depending on the illumination geometry of the flyby). We then correlated that 'best match' pixel on each flyby with its corresponding cylindrical map to find the best geometric matches to any given category of spectral unit (in this case, cloud). The T33 cloud at 40.1°S 142.9°E compares most favorably and is shown in Figure 20.

We used the same identical-i-e search algorithm to find appropriate surface spectra to compare the Hetpet Regio change at the bottom of Figure 20. The brightened spectrum is not a linear combination of the unchanged spectrum and either Xanadu (from T12, 4.3°N 116.7°W) or Tui Regio (from T46, 24.6°S 122.4°W). The brightened area shows particularly high I/F enhancement at 2.0 μm, an enhanced 2.8 μm/2.7 μm ratio, and less enhancement at 5.0 μm, which is a pattern in general agreement with that of Xanadu. But the change is under-bright with respect to Tui and Xanadu in the short-wavelength windows, 0.93 μm, 1.08 μm, 1.28 μm, and 1.6 μm, when compared to 2.0 μm and particularly 2.8 μm. Xanadu is the best candidate comparison spectrum, particularly if the discrepancies that we observe result from residual differences in the atmospheric contribution (particularly the phase angle).

We also performed direct comparison of the surface spectra of the brightened areas, with the caveat that it is challenging due to differing observing geometries. Figure 22 shows the spectra of the brightened areas in Yalaing Terra, Hetpet Regio, and Adiri. None of the brightening in Concordia Regio fills a full VIMS pixel from T77, so we exclude it. Despite differing observing geometries, the spectra agree with each other very well, particularly at long wavelengths where atmospheric influence is less important. In the short wavelength windows, aerosol scattering dominates over surface signal, particularly at high airmass. Therefore the departures from agreement at short wavelengths result from the atmosphere, not the surface brightening. Hence we infer that the brightening in each area is consistent with alteration to the same composition and that the same process is responsible for the brightening in each area.

Discussion

There are important constraints to glean from the observations that any proposed mechanism to explain these surface changes needs to meet:

1. Although our temporal coverage is incomplete, in at least some places the changed areas darken first, remain dark for a period of weeks to months, become brightened beyond their original equatorial bright state, and then the extents of the brightened areas slowly decrease over timescales of months to a year.
2. Brightening only occurs on Equatorial Bright terrains, never in dunes, mountains, or the VIMS dark blue unit despite the geographic proximity of those terrains to the brightened areas.
3. The brightenings are surficial features, inconsistent with both high altitude clouds and low-lying fog.
4. I/F increases at all wavelengths in brightened areas.
5. The spectra of brightened areas all match each other to within the uncertainty of measured surface reflectance, at least at wavelengths where such comparisons are valid.
6. One instance of evaporite in Yalaing Terra disappeared temporarily as a result of the event.
7. Early on, brightened areas exist contiguously with darkened areas.

The similarities in brightened spectra (constraint 5) along with the similarities of brightness histories

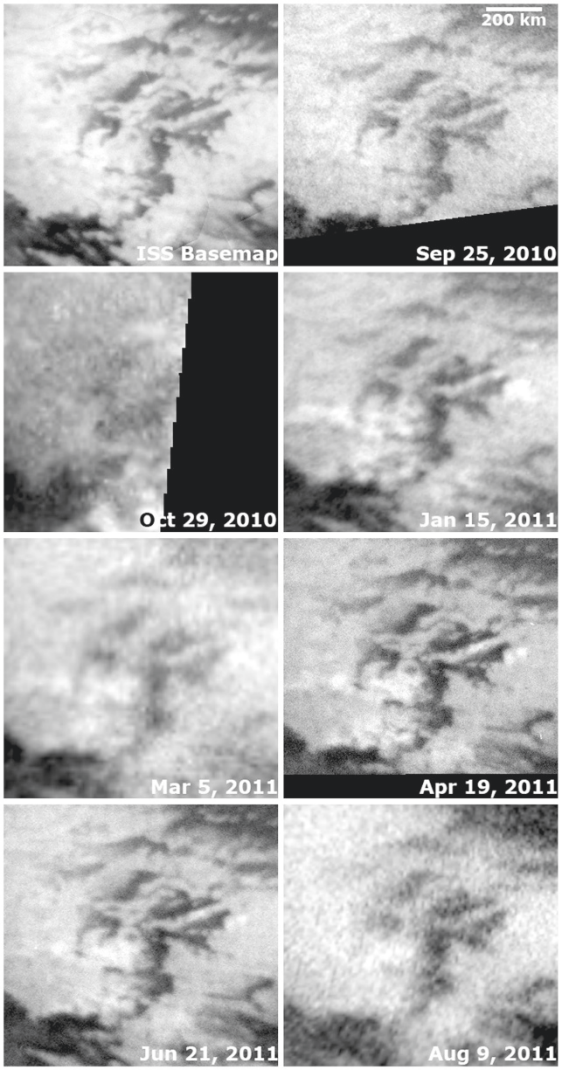

Figure 17 Adiri time evolution. *Cassini* ISS monitoring of the evolution of altered surface areas within Adiri from 2010 through 2011. These brightenings were initially reported by Turtle et al. 2011 [27] from the 2011 January 15 observation. After darkening in at least one of the areas right after the event on 2010 October 29, the pattern of brightening afterward shows an initially maximum extent that shrinks over the ensuing months. Some darkening of dunes occured between Adiri and Concordia Regio as well.

(constraint 1) together imply that we are looking at multiple instances of the same physical process. Moreover, the similarity in latitude, relative contiguity in longitude, cotemporal occurrence, and correlation with the 2010 cloudburst event identified by Turtle et al. 2011 [27] are all consistent with the process originating with some sort of precipitation.

Hence we concur that the surface-wetting hypothesis put forth by Turtle et al. 2011 [27] fits the initial surface darkening following the cloudburst. Such darkening occurs because wetting the surface changes the index of refraction of the surface layer increasing the probability of internal reflection [44], because the new refractive index reduces the intensity of first-surface and subsequent reflections [45], and because wetting softens rough edges, decreasing surface roughness at optical wavelengths [46]. Surface darkening due to precipitation wetting of the surface was first seen on Earth from Gemini 4 in 1965 [47,48] (Figure 23). Christophe Sotin et al. (in prep) experimentally verified that liquid hydrocarbons can wet ice at Titan-relevant temperatures and, furthermore, that such wetting leads to surface darkening not dissimilar from that seen on Earth from Gemini 4. Either spatially varying amounts of rainfall or varying capacity of the soil to retain moisture could lead to the geographic variability in surface response (constraint 7).

A potential problem with wetting by pure liquid methane comes from the evaporation rate. Mitri [49] estimates evaporation rates for 100% methane at 94 K exposed to a 1 m/s wind to be $\sim$ 15 meters per year, while for 35% methane, 60% ethane, 5% nitrogen it was estimated to be $\sim$ 6 meters per year. These translate to 2-5 mm/day. More detailed calculations [15,50] show that the Mitri calculation most likely represents an upper limit, and that evaporation rates on the order of $\sim$ 1 m per Titan year are more likely. The most trustworthy observations of continuous surface darkening are from Concordia Regio (Figure 14), where the darkening lasted for at least 80 days. An exposed solution would evaporate 1.6 meters of liquid in that time. However, that number would be decreased by the liquid's surface activity, given wetting, and reduced further by evaporative cooling of the liquid

Figure 18 Adiri changes. Titan's bright region Adiri (view centered $\sim$ 1000 km west of the *Huygens* Landing Site) as seen by VIMS both before (T31 and T70) and after (T75 and T77) the 2010 September 27 cloudburst event. Several discrete, separated areas of Equatorial Bright terrain brightened across the expanse of Adiri, as is evident from the view on T77. The T75 view has poor spatial resolution, but still shows evident brightening in the affected areas.

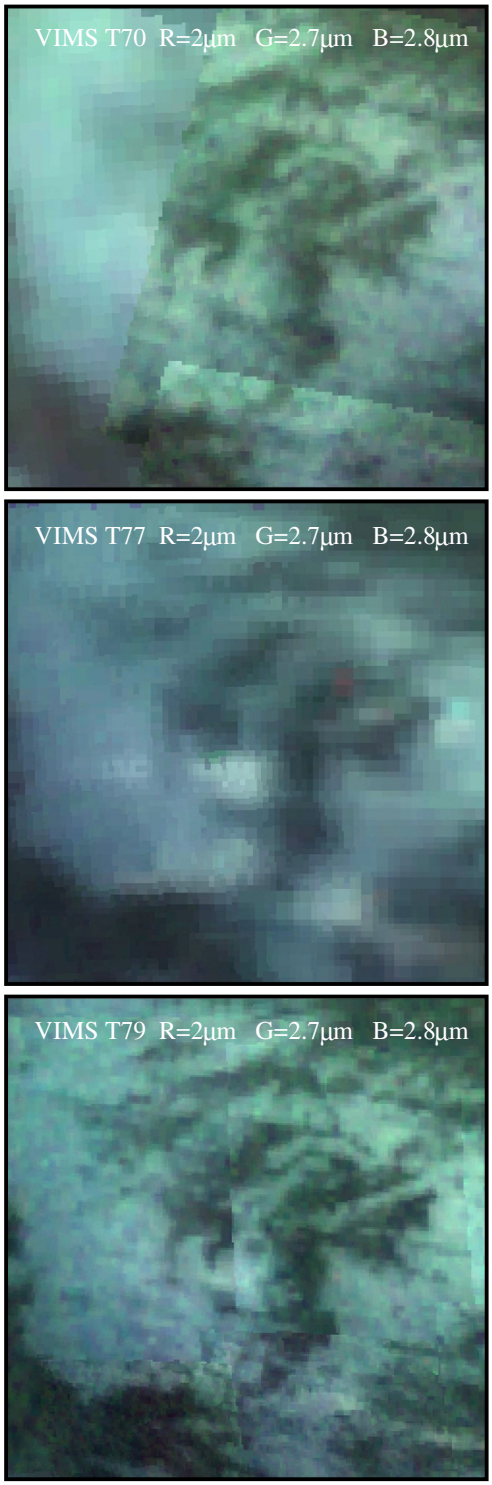

Figure 19 Adiri changes in doublepeak color. Titan's bright region Adiri (view centered ∼ 1000 km west of the *Huygens* Landing Site) as seen by VIMS over the time range discussed in the text. This color scheme, colormapped with red as 2.0μm, green as 2.7μm, and blue as 2.8um, accentuates the changed areas of the surface due to the relatively greater brightening at 2.0μm and 2.8μm in the observed spectra (Figure 20).

and solid surface [51]. Further numerical studies and/or experiments are needed characterize the process of a hydrocarbon-wetted icy surface drying due to evaporation on Titan.

The geologic context for the ensuing brightening – not in dunes or mountains, but rather in valleys (sometimes) adjacent to mountains – might relate to the nature of the surface. Rain on mountains might be expected to easily run off, whereas rain onto a porous regolith could penetrate in and wet the surface layer. Rain into dunes might then very easily percolate down far enough so as to be inaccessible from the surface.

The brightening lasted many months (over a year in Yalaing Terra and Hetpet Regio) before fading back to the original spectrum. That duration is inconsistent with chemical alterations to the surface. A chemical change to the surface associated with precipitation – say by rain washing the surface clean (as proposed for the origin of Xanadu [52]), physical overturn of the surface layer exposing fresh regolith, chemical weathering, or sediment deposition – would likely not return to the original spectrum so closely or so quickly. Deposition timescales for atmospheric haze [53,54] are estimated to be 0.1 μm per Titan year – too low to bury and overprint chemically altered surfaces.

Thus we conclude that the surface brightening that follows the precipitation-wetted and -darkened surface is probably the result of the presence of a transient layer of material – potentially a volatile. A volatile can both be emplaced and removed over the timescales shown by the observations. Any solid with small grain size would appear bright at all wavelengths to VIMS, and thus be consistent with the observed spectrum.

The composition and nature of such a volatile remains an open question. The *Huygens*-measured surface temperature in Titan's tropics was 93.65 $\pm$ 0.25 K [55] – well above the freezing point of both methane (90.7 K) and ethane (90.4 K). Hence, even if hail survived passage through Titan's lower atmosphere as a solid to land on the surface [26], the warm surface might eventually melt it. If that timescale is sufficiently short, less than a few weeks, then both solid and liquid precipitation might be expected to leave a darkened wetted surface like that seen by ISS. Given that we see the time progression of dark, then brightened, a simple hail or snow scenario is not consistent with the observations.

Some process then needs to occur that leaves a thin layer of solid on the surface.

One possible option would be dissolution, wicking upward, and subsequent reprecipitation of heavier hydrocarbons like acetylene or hydrogen cyanide on the surface. This process would be related to evaporite formation [11], but is sufficiently distinct as to the chemicals involved that it might reasonably be expected to lead to different surface

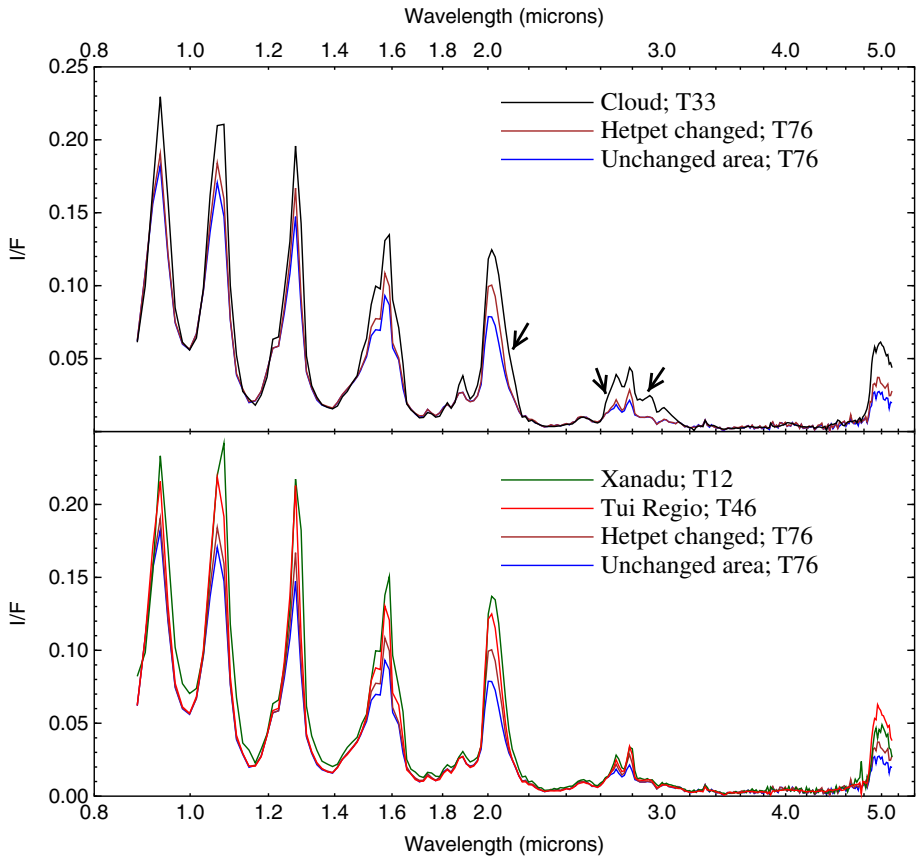

Figure 20 Spectral changes. In this figure we compare the VIMS spectra of Hetpet Regio both before (blue) and after (dark red) the brightening in the wake of the 2010 September 27 cloudburst. To minimize the effects of differing observation geometry on atmospheric effects, we used an area near the change area from the same flyby, T76, for the 'before' baseline. The two areas had identical spectra on T61, before the change event. We compare those spectra to that of a cloud from T33 at top and to Xanadu from T12 and Tui Regio from T46 at bottom. For intercomparability the cloud, Xanadu, and Tui pixels were chosen to have identical incidence and emission angles as Hetpet Regio on T76 (Xanadu had a different phase, leading to some differences in atmospheric contribution). The changed area spectrum is inconsistent with that of a cloud (see arrows), and likewise does not represent a linear combination of pre-changed spectrum and either Xanadu or Tui either.

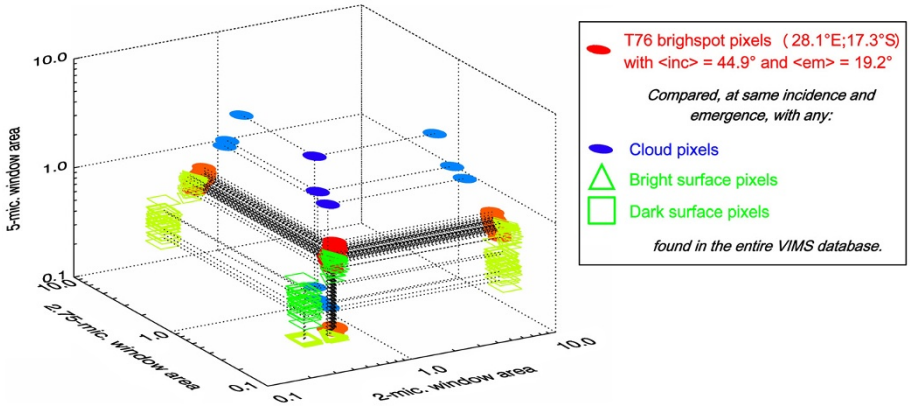

Figure 21 Spectral window changes. Here we compare the relative integrated *I*/*F* for clouds, bright terrain, dark terrain, and the T76 Yalaing Terra brightened terrain within the spectral windows and acquired under the same viewing geometry with i=45°, e=19°. This three-dimensional plot shows the total spectral areas for individual pixels in each of these terrains, integrated across the 2, 2.68/2.78, and 5 micron windows. The T76 brightened surfaces plot apart from both dark and bright terrain, and well apart from clouds.

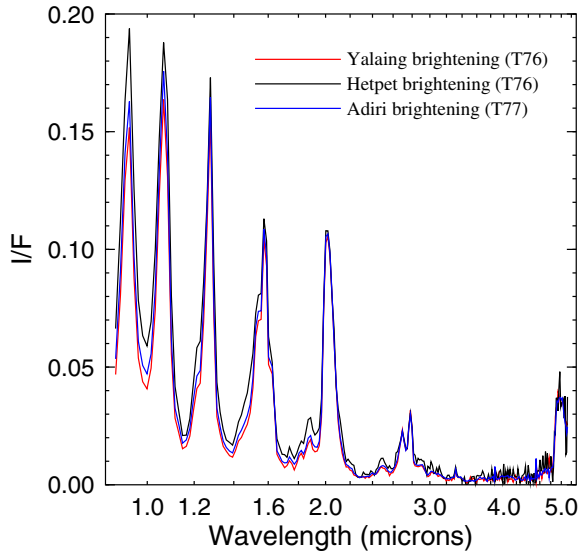

Figure 22 Brightening comparison. Here we directly compare the spectra of the brightened surfaces from Yalaing Terra (i=40°, e=21°, ϕ=42°), Hetpet Regio (i=32°, e=55°, ϕ=45°), and Adiri (i=34°, e=15°, ϕ=20°). We exclude Concordia Regio due to the coarse VIMS spatial resultion there on T77 in which the brightened area fills less than a full pixel. Because the viewing geometries differ significantly, no accurate quantitative comparison is possible – particularly at short wavelengths. However the spectra agree with one another quite well, particularly at longer wavelengths where viewing geometry through the atmosphere plays a lesser role. Within the short-wavelength windows, 0.93 μm, 1.08 μm, and 1.28 μm, atmospheric scattering leads to the apparent differences in I/F.

spectra from the lake-bottom evaporites. The crystals of such precipitates could sinter together over time to increase the grain size and revert the surface to its previous state. Initial calculations using a model that assumes ice grain growth by vapor exchange (after [56]) indicate that propane (for example) would take weeks to months to coalesce, and is therefore a credible candidate. Here we assume that evaporative cooling keeps propane as ice (its melting point is 85.5 K). Solids with melting points signficantly above ambient Titan temperatures, like acetylene and butane, would take several years and a thousand years respectively for grain growth – inconsistent with the observed reversion time that is on the order of months to a year.

Scenarios involving subsurface percolation of liquid might be expected to not be possible in rocky areas without surficial regolith, or in extremely porous media like sand. Hence this could explain the geographical confinement of brightening to Equatorial Bright terrain.

The evaporative cooling scenario would necessarily involve surface temperatures $\lesssim$ 90 K. A thermal signature of the resulting surface cold spots might then be visible to the Cassini InfraRed Spectrometer (CIRS) instrument, which has measured Titan surface temperatures previously [57,58]. Unfortunately no CIRS observations exist that are sufficient to constrain surface temperatures of the changed areas in the relevant timeframe (2010 September to 2011 December; V. Cottini, personal communication).

Another possibility is that the precipitated liquid itself freezes on the surface due to evaporative cooling. In this scenario, evaporation subsequent to the initial wetting continually cools the surface, with a cooling thermal wave propagating into the surface via conduction. Evaporative cooling can be tremendously efficient, as any swimmer leaving a swimming pool on a windy day in the desert will experience. After some or most of the near-surface liquid is evaporated away, the surface temperature could drop below the freezing point, resulting in a thin frost that then sublimes away over the course of the ensuing months. Alternately, if the structures left on the surface are sufficiently fragile then wind might be able to erode them away by wind entrainment over time.

The chemical identity of such evaporatively cooled frost would probably be methane, ethane, or a solution of methane and ethane. Graves [26] suggested two possible composition models for Titan's rain, which wetted the surface in the first place: 40% methane, 40% ethane, 20% dissolved nitrogen (assuming 50% relative humidity for ethane); and 77% methane, 23% nitrogen (with 0% ethane relative humidity). Graves [26] predicted that ethane-rich drops would be warm when they reached the ground (93.5 K), but methane-nitrogen drops would be cold due to evaporative cooling (90.0 K). Hence a surface wetted by methane-nitrogen drops would evaporate methane and cool off and might continue to do so until the surface temperature becomes cold enough to freeze the liquid as its composition evolves. In the context of lakes, modeling has shown that a pure-methane lake would freeze due to evaporative cooling under polar conditions [49,51].

Alternatively, the nearly pure methane hail that Graves [26] suggests might be able to both cool the surface significantly on its initial melting, and to increase the freezing point of the liquid due to exsolution of nitrogen from the hailstone on freezing.

This evaporative-cooling/frost hypothesis is consistent with the observational data. Clearly, however, additional thinking, modeling, and experimentation would be needed to verify whether or not it is indeed plausible under Titan conditions. More comprehensive work might also be able to constrain possible compositions for the resulting frost. If surface temperature measurements were sufficiently precise, they might also be able to test the model by directly determining temperatures in affected areas before, during, and after a rainfall event.

An alternate scenario for the origin and disappearance of the thin, brightened surface layer involves purely physical processes. On Earth, some types of terrain will

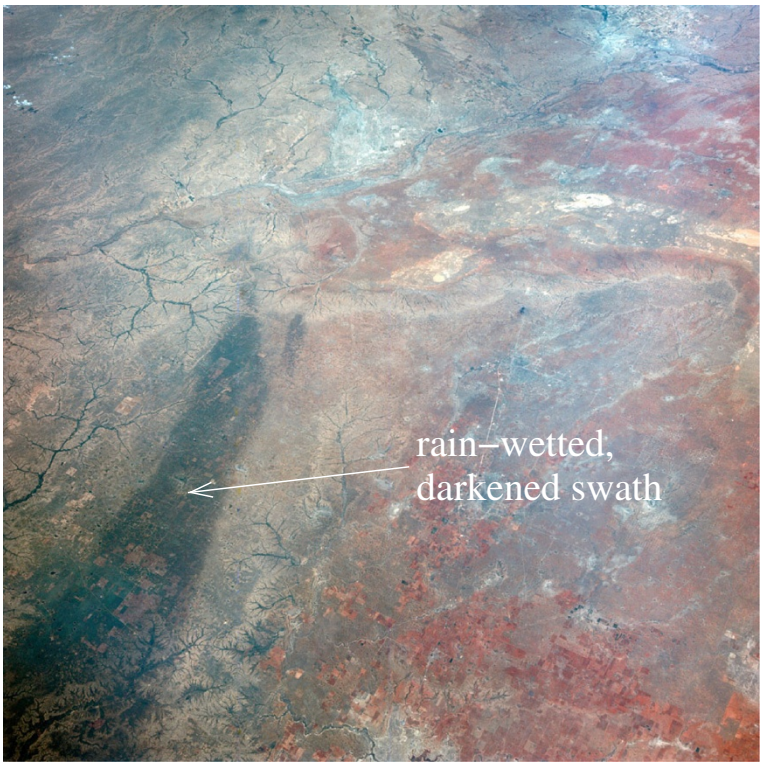

Figure 23 Rainfall darkening from Gemini 4 image of northern Texas, USA from the Gemini 4 spacecraft in 1965 June [47]. This image shows a swath of ground that was darkened by wetting in a local thunderstorm, as documented by ground-based meteorological stations [48]. Image courtesy of the Image Science & Analysis Laboratory, NASA Johnson Space Center, Mission: GEM04 Roll: 8 Frame: 34702 http://eol.jsc.nasa.gov.

typically develop a very thin deposit of bright, fine-grained material in the wake of rain storms. This deposit is composed of local materials that were remobilized by the presence of liquid. On Titan, such a layer could develop rapidly upon drying, and then disappear as the fine-grained material blows away due to aeolian erosion.

Conclusion

We analyze the surface reflectivity history of four study areas on Titan in the wake of the 2010 September cloudburst storm: Yalaing Terra, Hetpet Regio, Concordia Regio, and Adiri. *Cassini* ISS shows that these areas darkened in the wake of the storm due to wetting of the surface regolith by rainfall [27]. Weeks to months later, each of these areas showed patches of significant and extensive surface brightening that persisted for up to a year before reverting to their previous spectrum.

Each of these areas had been completely static for the entirety of the mission up until the 2010 September cloudburst. Their temporal co-association along with the narrow latitude range and large longitude range (120°) indicates that the surface changes, both darkening and brightening, are associated with precipitation.

Near-infrared spectral mapping from VIMS observations of the affected areas shows that the brightening occurred at all wavelengths and was uniform across the four study areas. The cloud wings and the in-window I/F measured rule out an atmospheric source for the brightening. The spectrally uniform ('white') brightening is consistent with either full or patchy deposition of a fine-grained solid.

The physical process that led to the brightening might be deposition of a thin layer of volatile frost. Multiple pathways for generating such a layer are possible. One is that cooling via methane evaporation might freeze either a component of the liquid itself or condense atmospheric gases out on to the surface. The volatile layer then sublimates over the ensuing year.

Alternatively, fine remobilized grains could generate the brighened surface layer. In this scenario, the fine grains would blow away over time in order to allow the surface to revert to its original spectrum.

Analysis of RADAR overlap with the Adiri study area shows that the brightenings do not occur within mountain or dune units, but rather only occur in VIMS Equatorial Bright terrain between mountains. This geologic correlation could result from differences in regolith properties or the local liquid (hydrocarbon) table.

Future work needs to be done to either constrain or rule out various brightening mechanisms. Computer models

and/or laboratory work could significantly contribute to our understanding of the brightening's origin. Furthermore, continued monitoring by *Cassini*'s instruments will be able to identify future instances of surface changes and, by using comparison with the events described here, to further constrain the deposition process and Titan's volatile cycle.

Competing interests
The authors declare that they have no competing interests.

Authors' contributions
RHB, BJB, KHB, CS, TBM, RNC, and PDN designed the VIMS instrument and planned observations. JWB, BJB, JB, PAD, RHB, SR, SLM, POH, JMS, and LAS executed the primary VIMS spectral analyses. EPT and JP provided and interpreted ISS observations. JWB, BJB, EPT, RHB, RDL, MJM, JMS, and LAS contributed interpretations of the observations. JWB wrote the manuscript. All authors read and approved the final manuscript.

Acknowledgements
The authors acknowledge support from the NASA/ESA *Cassini* Project. JWB acknowledges support from NASA Outer Planets Research Program grant NNX10AQ10G.

Author details
[1]Department of Physics, University of Idaho, Moscow, Idaho, 83844-0903 USA. [2]Jet Propulsion Laboratory, Caltech, Pasadena, California, 91109 USA. [3]University of California, Berkeley, California, 94720 USA. [4]Bear Fight Institute, Winthrop, Washington, 98862 USA. [5]Lunar and Planetary Laboratory, University of Arizona, Tucson, Arizona, 85721 USA. [6]United States Geological Survey, Denver, Colorado, 80225 USA. [7]Division of Geological and Planetary Sciences, California Institute of Technology, Pasadena, CA 91126 USA. [8]Laboratoire de Planétologie et Géodynamique, CNRS UMR6112, Université de Nantes, Nantes, France. [9]Department of Astronomy, Cornell University, Ithaca, NY 14853 USA. [10]Laboratoire AIM, Université Paris Diderot / CEA Irfu / CNRS, Centre de l'orme des Mérisiers, bât. 709, 91191 Gif/Yvette Cedex, France. [11]Astrogeology Division, United States Geological Survey, Flagstaff, Arizona 86001 USA. [12]DLR, Institute of Planetary Research, 12489 Berlin, Germany. [13]Johns Hopkins University Applied Physics Laboratory, Laurel, MD 20723 USA. [14]Department of Earth and Atmospheric Science, Massachusetts Institute of Technology, Cambridge, MA 02141 USA. [15]Space Science and Engineering Center, University of Wisconsin, Madison, WI 53706 USA.

Received: 17 March 2012 Accepted: 29 October 2012
Published: 14 January 2013

References

1. Soderblom LA, Tomasko MG, Archinal BA, Becker TL, Bushroe MW, Cook DA, Doose LR, Galuszka DM, Hare TM, Howington-Kraus E, Karkoschka E, Kirk RL, Lunine JI, McFarlane EA, Redding BL, Rizk B, Rosiek MR, See C, Smith PH: **Topography and geomorphology of the Huygens landing site on Titan.** *Planet Space Sci* 2007, **55:**2015–2024.
2. Porco CC, Baker E, Barbara J, Beurle K, Brahic A, Burns JA, Charnoz S, Cooper N, Dawson DD, Del Genio AD, Denk T, Dones L, Dyudina U, Evans MW, Fussner S, Giese B, Grazier K, Helfenstein P, Ingersoll AP, Jacobson RA, Johnson TV, McEwen A, Murray CD, Neukum G, Owen WM, Perry J, Roatsch T, Spitale J, Squyres S, Thomas P, Tiscareno M, Turtle EP, Vasavada AR, Veverka J, Wagner R, West R: **Imaging of Titan from the Cassini spacecraft.** *Nature* 2005, **434:**159–168.
3. Barnes JW, Radebaugh J, Brown RH, Wall S, Soderblom L, Lunine J, Burr D, Sotin C, Le Mouélic S, Rodriguez S, Buratti B J, Clark R, Baines KH, Jaumann R, Nicholson PD, Kirk RL, Lopes R, Lorenz RD, Mitchell K, Wood CA: **Near-infrared spectral mapping of Titan's mountains and channels.** *J Geophysical Res (Planets)* 2007, **112:**E11006.
4. Lorenz RD, Lopes RM, Paganelli F, Lunine JI, Kirk RL, Mitchell KL, Soderblom LA, Stofan ER, Ori G, Myers M, Miyamoto H, Radebaugh J, Stiles B, Wall SD, Wood CA: **Fluvial channels on Titan: initial Cassini RADAR observations.** *Planet Space Sci* 2008, **56:**1132–1144.
5. Jaumann R, Brown RH, Stephan K, Barnes JW, Soderblom LA, Sotin C, Le Mouélic S, Clark RN, Soderblom J, Buratti BJ, Wagner R, McCord TB, Rodriguez S, Baines KH, Cruikshank DP, Nicholson PD, Griffith CA, Langhans M, Lorenz RD: **Fluvial erosion and post-erosional processes on Titan.** *Icarus* 2008, **197:**526–538.
6. Burr DM, Jacobsen RE, Roth DL, Phillips CB, Mitchell KL, Viola D: **Fluvial network analysis on Titan: evidence for subsurface structures and west-to-east wind flow, southwestern Xanadu.** *Geophys Res Lett* 2009, **36:**L22203.
7. Langhans MH, Jaumann R, Stephan K, Brown RH, Buratti BJ, Clark RN, Baines KH, Nicholson PD, Lorenz RD, Soderblom LA, Soderblom JM, Sotin C, Barnes JW, Nelson R: **Titan's fluvial valleys: Morphology, distribution, and spectral properties.** *Planet Space Sci* 2012, **60:**34–51.
8. Stofan ER, Elachi C, Lunine JI, Lorenz RD, Stiles B, Mitchell KL, Ostro S, Soderblom L, Wood C, Zebker H, Wall S, Janssen M, Kirk R, Lopes R, Paganelli F, Radebaugh J, Wye L, Anderson Y, Allison M, Boehmer R, Callahan P, Encrenaz P, Flamini E, Francescetti G, Gim Y, Hamilton G, Hensley S, Johnson WTK, Kelleher K, Muhleman D, Paillou P, Picardi G, Posa F, Roth L, Seu R, Shaffer S, Vetrella S, West R: **The lakes of Titan.** *Nature* 2007, **445:**61–64.
9. Brown RH, Soderblom LA, Soderblom JM, Clark RN, Jaumann R, Barnes JW, Sotin C, Buratti B, Baines KH, Nicholson PD: **The identification of liquid ethane in Titan's Ontario Lacus.** *Nature* 2008, **454:**607–610.
10. Hayes A, Aharonson O, Callahan P, Elachi C, Gim Y, Kirk R, Lewis K, Lopes R, Lorenz R, Lunine J, Mitchell K, Mitri G, Stofan E, Wall S: **Hydrocarbon lakes on Titan: Distribution and interaction with a porous regolith.** *Geophysical Res Lett* 2008, **35:**L9204.
11. Barnes JW, Bow J, Schwartz J, Brown RH, Soderblom JM, Hayes AG, Vixie G, Le Mouélic S, Rodriguez S, Sotin C, Jaumann R, Stephan K, Soderblom LA, Clark RN, Buratti BJ, Baines KH, Nicholson PD: **Organic sedimentary deposits in Titan's dry lakebeds: Probable evaporite.** *Icarus* 2011, **216:**136–140.
12. Strobel DF: **The photochemistry of hydrocarbons in the atmosphere of Titan.** *Icarus* 1974, **21:**466.
13. Yung YL, Allen M, Pinto JP: **Photochemistry of the atmosphere of Titan - comparison between model and observations.** *ApJS* 1984, **55:**465–506.
14. Rannou P, Montmessin F, Hourdin F, Lebonnois S: **The latitudinal distribution of clouds on Titan.** *Science* 2006, **311:**201–205.
15. Mitchell JL: **The drying of Titan's dunes: Titan's methane hydrology and its impact on atmospheric circulation.** *J Geophysical Res (Planets)* 2008, **113:**8015.
16. Lorenz RD, Wall S, Radebaugh J, Boubin G, Reffet E, Janssen M, Stofan E, Lopes R, Kirk R, Elachi C, Lunine J, Mitchell K, Paganelli F, Soderblom L, Wood C, Wye L, Zebker H, Anderson Y, Ostro S, Allison M, Boehmer R, Callahan P, Encrenaz P, Ori GG, Francescetti G, Gim Y, Hamilton G, Hensley S, Johnson W, Kelleher K, Muhleman D, Picardi G, Posa F, Roth L, Seu R, Shaffer S, Stiles B, Vetrella S, Flamini E, West R: **The sand seas of Titan: Cassini RADAR observations of longitudinal dunes.** *Science* 2006, **312:**724–727.
17. Lorenz RD, Radebaugh J: **Global pattern of Titan's dunes: Radar survey from the Cassini prime mission.** *Geophys Res Lett* 2009, **36:**L3202.
18. Niemann HB, Atreya SK, Bauer SJ, Carignan GR, Demick JE, Frost RL, Gautier D, Haberman JA, Harpold DN, Hunten DM, Israel G, Lunine JI, Kasprzak WT, Owen TC, Paulkovich M, Raulin F, Raaen E, Way SH: **The abundances of constituents of Titan's atmosphere from the GCMS instrument on the Huygens probe.** *Nature* 2005, **438:**779–784.
19. Lorenz RD, Niemann HB, Harpold DN, Way SH, Zarnecki JC: **Titan's damp ground: constraints on Titan surface thermal properties from the temperature evolution of the Huygens GCMS inlet.** *Meteoritics Planetary Sci* 2006, **41:**1705–1714.
20. Karkoschka E, Tomasko MG: **Rain and dewdrops on titan based on in situ imaging.** *Icarus* 2009, **199:**442–448.
21. Rodriguez S, Le Mouélic S, Rannou P, Tobie G, Baines KH, Barnes JW, Griffith CA, Hirtzig M, Pitman KM, Sotin C, Brown RH, Buratti BJ, Clark RN, Nicholson PD: **Global circulation as the main source of cloud activity on Titan.** *Nature* 2009, **459:**678–682.
22. Brown ME, Roberts JE, Schaller EL: **Clouds on Titan during the Cassini prime mission: a complete analysis of the VIMS data.** *Icarus* 2010, **205:**571–580.

23. Rodriguez S, Le Mouélic S, Rannou P, Sotin C, Brown RH, Barnes JW, Griffith CA, Burgalat J, Baines KH, Buratti BJ, Clark RN, Nicholson PD: **Titan's cloud seasonal activity from winter to spring with Cassini/VIMS.** *Icarus* 2011, **216:**89–110.
24. Turtle EP, Del Genio AD, Barbara JM, Perry JE, Schaller EL, McEwen AS, West RA, Ray TL: **Seasonal changes in Titan's meteorology.** *Geophys Res Lett* 2011, **38:**L03203.
25. Lorenz RD: **The life, death and afterlife of a raindrop on Titan.** *Planet Space Sci* 1993, **41:**647–655.
26. Graves SDB, McKay CP, Griffith CA, Ferri F, Fulchignoni M: **Rain and hail can reach the surface of Titan.** *Planet Space Sci* 2008, **56:**346–357.
27. Turtle EP, Perry JE, Hayes AG, Lorenz RD, Barnes JW, McEwen AS, West RA, Del Genio AD, Barbara JM, Lunine JI, Schaller EL, Ray TL, Lopes RMC, Stofan ER: **Rapid and extensive surface changes near Titan's equator: evidence of april showers.** *Science* 2011, **331:**1414–1417.
28. Brown RH, Baines KH, Bellucci G, Bibring JP, Buratti BJ, Capaccioni F, Cerroni P, Clark RN, Coradini A, Cruikshank DP, Drossart P, Formisano V, Jaumann R, Langevin Y, Matson DL, McCord TB, Mennella V, Miller E, Nelson RM, Nicholson PD, Sicardy B, Sotin C: **The Cassini Visual and infrared mapping spectrometer (Vims) investigation.** *Space Sci Rev* 2004, **115:**111–168.
29. Porco CC, West RA, Squyres S, McEwen A, Thomas P, Murray CD, Delgenio A, Ingersoll AP, Johnson TV, Neukum G, Veverka J, Dones L, Brahic A, Burns JA, Haemmerle V, Knowles B, Dawson D, Roatsch T, Beurle K, Owen W: **Cassini imaging science: instrument characteristics and anticipated scientific investigations at Saturn.** *Space Sci Rev* 2004, **115:** 363–497.
30. Elachi C, Allison MD, Borgarelli L, Encrenaz P, Im E, Janssen MA, Johnson WTK, Kirk RL, Lorenz RD, Lunine JI, Muhleman DO, Ostro SJ, Picardi G, Posa F, Rapley CG, Roth LE, Seu R, Soderblom LA, Vetrella S, Wall SD, Wood CA, Zebker HA: **Radar: the Cassini Titan radar mapper.** *Space Sci Rev* 2004, **115:**71–110.
31. Barnes JW, Brown RH, Soderblom L, Buratti BJ, Sotin C, Rodriguez S, Le Mouèlic S, Baines KH, Clark R, Nicholson P: **Global-scale surface spectral variations on Titan seen from Cassini/VIMS.** *Icarus* 2007, **186:** 242–258.
32. Turtle EP, Perry JE, McEwen AS, Del Genio AD, Barbara J, West RA, Dawson DD, Porco CC: **Cassini imaging of Titan's high-latitude lakes, clouds, and south-polar surface changes.** *Geophysical Res Lett* 2009, **36:**L2204.
33. Buratti BJ, Sotin C, Brown RH, Hicks MD, Clark RN, Mosher JA, McCord TB, Jaumann R, Baines KH, Nicholson PD, Momary T, Simonelli DP, Sicardy B: **Titan: preliminary results on surface properties and photometry from VIMS observations of the early flybys.** *Planet Space Sci* 2006, **54:**1498–1509.
34. Radebaugh J, Lorenz RD, Lunine JI, Wall SD, Boubin G, Reffet E, Kirk RL, Lopes RM, Stofan ER, Soderblom L, Allison M, Janssen M, Paillou P, Callahan P, Spencer C: **The Cassini Radar Team: Dunes on Titan observed by Cassini radar.** *Icarus* 2008, **194:**690–703.
35. Rodriguez S, Le Mouélic S, Sotin C, Clénet H, Clark RN, Buratti B, Brown RH, McCord TB, Nicholson PD, Baines KH, the VIMS Science Team: **Cassini/VIMS hyperspectral observations of the HUYGENS landing site on Titan.** *Planet Space Sci* 2006, **54:**1510–1523.
36. Barnes JW, Brown RH, Turtle EP, McEwen AS, Lorenz RD, Janssen M, Schaller EL, Brown ME, Buratti BJ, Sotin C, Griffith C, Clark R, Perry J, Fussner S, Barbara J, West R, Elachi C, Bouchez AH, Roe HG, Baines KH, Bellucci G, Bibring JP, Capaccioni F, Cerroni P, Combes M, Coradini A, Cruikshank DP, Drossart P, Formisano V, Jaumann R, Langevin Y, Matson DL, McCord TB, Nicholson PD, Sicardy B: **A 5-Micron-Bright spot on Titan: evidence for surface diversity.** *Science* 2005, **310:**92–95.
37. McCord TB, Hansen GB, Buratti BJ, Clark RN, Cruikshank DP, D'Aversa E, Griffith CA, Baines EKH, Brown RH, Dalle Ore CM, Filacchione G, Formisano V, Hibbitts CA, Jaumann R, Lunine JI, Nelson RM, Sotin C, the Cassini VIMS Team: **Composition of Titan's surface from Cassini VIMS.** *Planet Space Sci* 2006, **54:**1524–1539.
38. Barnes JW, Brown RH, Radebaugh J, Buratti BJ, Sotin C, Le Mouelic S, Rodriguez S, Turtle EP, Perry J, Clark R, Baines KH, Nicholson PD: **Cassini observations of flow-like features in western Tui Regio, Titan.** *Geophys Res Lett* 2006, **33:**L16204.
39. Barnes JW, Soderblom JM, Brown RH, Buratti BJ, Sotin C, Baines KH, Clark RN, Jaumann R, McCord TB, Nelson R, Le Mouélic S, Rodriguez S, Griffith C, Penteado P, Tosi F, Pitman KM, Soderblom L, Stephan K, Hayne P, Vixie G, Bibring J, Bellucci G, Capaccioni F, Cerroni P, Coradini A, Cruikshank DP, Drossart P, Formisano V, Langevin Y, Matson DL, Nicholson PD, Sicardy B: **VIMS spectral mapping observations of Titan during the Cassini prime mission.** *Planetary Space Sci* 2009, **57:**1950–1962.
40. Lunine JI, Elachi C, Wall SD, Janssen MA, Allison MD, Anderson Y, Boehmer R, Callahan P, Encrenaz P, Flamini E, Franceschetti G, Gim Y, Hamilton G, Hensley S, Johnson WTK, Kelleher K, Kirk RL, Lopes RM, Lorenz R, Muhleman DO, Orosei R, Ostro SJ, Paganelli F, Paillou P, Picardi G, Posa F, Radebaugh J, Roth LE, Seu R, Shaffer S, Soderblom LA, Stiles B, Stofan ER, Vetrella S, West R, Wood CA, Wye L, Zebker H, Alberti G, Karkoschka E, Rizk B, McFarlane E, See C, Kazeminejad B: **Titan's diverse landscapes as evidenced by Cassini RADAR's third and fourth looks at Titan.** *Icarus* 2008, **195:**415–433.
41. Radebaugh J, Lorenz RD, Kirk RL, Lunine JI, Stofan ER, Lopes RMC, Wall SD, the Cassini Radar Team: **Mountains on Titan observed by Cassini Radar.** *Icarus* 2007, **192:**77–91.
42. Perry JE, McEwen AS, Fussner S, Turtle EP, West RA, Porco CC, Knowles B, Dawson DD, Cassini Iss Team: **Processing ISS Images of Titan's Surface.** In *36th Annual Lunar and Planetary Science Conference, Volume 36 of Lunar and Planetary Institute Science Conference Abstracts*. Edited by Mackwell S, Stansbery E; 2005:2312.
43. Griffith CA, Penteado P, Baines K, Drossart P, Barnes J, Bellucci G, Bibring J, Brown R, Buratti B, Capaccioni F, Cerroni P, Clark R, Combes M, Coradini A, Cruikshank D, Formisano V, Jaumann R, Langevin Y, Matson D, McCord T, Mennella V, Nelson R, Nicholson P, Sicardy B, Sotin C, Soderblom LA, Kursinski R: **The evolution of Titan's mid-latitude clouds.** *Science* 2005, **310:**474–477.
44. Twomey SA, Bohren CF, Mergenthaler JL: **Reflectance and albedo differences between wet and dry surfaces.** *Appl Opt* 1988, **27**(7):1278–1280.
45. Lekner J, Dorf MC: **Why some things are darker when wet.** *Appl Opt* 1988, **27**(7):1278–1280.
46. Zhang H, Voss KJ: **Bidirectional reflectance study on dry, wet, and submerged particulate layers: effects of pore liquid refractive index and translucent particle concentrations.** *Appl Opt* 2006, **45**(34):8753–8763.
47. Nagler KM, Soules SD: **Cloud Photography from the Gemini 4 Spaceflight.** *Bull Am Meteorological Soc* 1965, **46:**522–527.
48. Hope JR: **Path of Heavy Rainfall Photographed from Space.** *Bull Am Meteorological Soc* 1966, **47:**371–373.
49. Mitri G, Showman AP, Lunine JI, Lorenz RD: **Hydrocarbon lakes on Titan.** *Icarus* 2007, **186:**385–394.
50. Schneider T, Graves SDB, Schaller EL, Brown ME: **Polar methane accumulation and rainstorms on Titan from simulations of the methane cycle.** *Nature* 2012, **481:**58–61.
51. Tokano T: **Limnological Structure of Titan's hydrocarbon lakes and its astrobiological implication.** *Astrobiology* 2009, **9:**147–164.
52. Smith PH, Lemmon MT, Lorenz RD, Sromovsky LA, Caldwell JJ, Allison MD: **Titan's surface, revealed by HST imaging.** *Icarus* 1996, **119:**336–349.
53. Toon OB, Turco RP, Pollack JB: **A physical model of Titan's clouds.** *Icarus* 1980, **43:**260–282.
54. Rannou P, Hourdin F, McKay CP: **A wind origin for Titan's haze structure.** *Nature* 2002, **418:**853–856.
55. Fulchignoni M, Ferri F, Angrilli F, Ball AJ, Bar-Nun A, Barucci MA, Bettanini C, Bianchini G, Borucki W, Colombatti G, Coradini M, Coustenis A, Debei S, Falkner P, Fanti G, Flamini E, Gaborit V, Grard R, Hamelin M, Harri AM, Hathi B, Jernej I, Leese MR, Lehto A, Lion Stoppato, P F, López-Moreno JJ, Mäkinen T, McDonnell JAM, McKay CP, Molina-Cuberos G, Neubauer FM, Pirronello V, Rodrigo R, Saggin B, Schwingenschuh K, Seiff A, Simões F, Svedhem H, Tokano T, Towner MC, Trautner R, Withers P, Zarnecki JC: **In situ measurements of the physical characteristics of Titan's environment.** *Nature* 2005, **438:**785–791.
56. Clark RN, Fraser PF, Aaron PZ: **Frost grain size metamorphism: Implications for remote sensing of planetary surfaces.** *Icarus* 1983, **56**(2):233–245.

57. Jennings DE, Cottini V, Nixon CA, Flasar FM, Kunde VG, Samuelson RE, Romani PN, Hesman BE, Carlson RC, Gorius NJP, Coustenis A, Tokano T: **Seasonal changes in Titan's surface temperatures.** *ApJ* 2011, **737:**L15.
58. Cottini V, Nixon CA, Jennings DE, de Kok R, Teanby NA, Irwin PGJ, Flasar FM: **Spatial and temporal variations in Titan's surface temperatures from Cassini CIRS observations.** *Planet Space Sci* 2012, **60:**62–71.

doi:10.1186/2191-2521-2-1
Cite this article as: Barnes *et al.*: Precipitation-induced surface brightenings seen on Titan by Cassini VIMS and ISS. *Planetary Science* 2013 **2**:1.